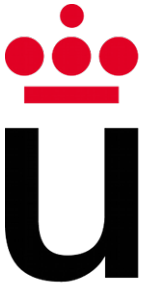

Universidad
Rey Juan Carlos

GRADO EN INGENIERÍA AEROESPACIAL EN AERONAVEGACIÓN

Curso Académico 2022/2023

Trabajo Fin de Grado

Exploration of vision-based control solutions for PX4-driven UAVs

Autora : Laura González Fernández
Tutores : Xin Chen, Alejandro Sáez Mollejo

Trabajo Fin de Grado

Exploration of Vision-Based Control Solutions for PX4-Driven UAVs.

Autora : Laura González Fernández
Tutores : Xin Chen, Alejandro Sáez Mollejo

La defensa del presente Proyecto Fin de Grado/Máster se realizó el día 3 de de 20XX, siendo calificada por el siguiente tribunal:

Presidente:

Secretario:

Vocal:

y habiendo obtenido la siguiente calificación:

Calificación:

Móstoles/Fuenlabrada, a de de 20XX

Aquí normalmente
se inserta una dedicatoria corta

Agradecimientos

Aquí vienen los agradecimientos...

Hay más espacio para explayarse y explicar a quién agradeces su apoyo o ayuda para haber acabado el proyecto: familia, pareja, amigos, compañeros de clase...

También hay quien, en algunos casos, hasta agradecer a su tutor o tutores del proyecto la ayuda prestada...

Resumen

Aquí viene un resumen del proyecto. Ha de constar de tres o cuatro párrafos, donde se presente de manera clara y concisa de qué va el proyecto. Han de quedar respondidas las siguientes preguntas:

- ¿De qué va este proyecto? ¿Cuál es su objetivo principal?
- ¿Cómo se ha realizado? ¿Qué tecnologías están involucradas?
- ¿En qué contexto se ha realizado el proyecto? ¿Es un proyecto dentro de un marco general?

Lo mejor es escribir el resumen al final.

Abstract

The popular open-source platform PX4 aims to facilitate the programming of unmanned aerial vehicles and their integration with new sensors and actuators and make it approachable for the common developer. This thesis aims to demonstrate how this platform can be used to develop solutions that integrate computer vision techniques and use their input to control the movement of an aerial vehicle, while employing easily-available and affordable hardware with basic specifications. For this purpose, a viable solution is presented that allows a drone to use an onboard camera to identify and keep track of a person in its field of view to follow their movement.

Todo list

TODO LIST

Contents

ListofFigures

List of Listings

Chapter 1

Introduction

1.1 General context

An Unmanned Aerial Vehicle (UAV) is an aircraft able to fly without any pilot or operator on board. They may be operated through remote control by a human operator or with various degrees of autonomy, from sensor-driven control aids provided to the operator to fully autonomous flight through preplanned missions. UAVs have existed since the 20th century and were initially developed as military technology to protect pilots from dangerous missions. However, as the cost of the electronics and sensors decreased and control technologies were improved, they became available to a broader public and are now employed in a wide range of civil applications like crop control, search and rescue, or filmmaking and photography. Nevertheless, most commercial solutions are limited to remote operations or basic autonomy, with fully autonomous flight still in the earliest phases. However, there is a growing trend towards using vision-based control solutions, which can offer improved performance and flexibility compared to traditional control methods. Vision-based control solutions use cameras and image processing algorithms to provide real-time feedback and control of the UAV. These solutions are often more flexible and robust than traditional control methods, which are typically based on accelerometers, gyroscopes, and other sensors. Additionally, vision-based control solutions can be implemented on low-cost platforms, making them accessible to a wider range of users. These vision-based guidance systems have only started to appear in recent years as artificial intelligence becomes more widespread and very few fully-developed consumer-ready platforms are available for the general public. Even so, from the essential hardware to build your own quadcopter, a helicopter with four rotors that represents the most common type of UAV, to miniaturized computers that handle complex calculations and open-source software that can be customized to endless applications, all the individual pieces that enable building such a system are readily available.

1.2 The Dronecontrol project

The project presented in this thesis aims to show the options available to design and implement control solutions for the popular PX4 open-source autopilot platform and how to integrate them with detection and tracking computer vision mechanisms to achieve simple vision-based self-guided UAVs. All the necessary code for this project has been written in the Python programming language and always runs outside of the flight controller board on a companion computer. This allows more processing power to be accessible for any compute-intensive computer vision algorithms, but also ensures that the control solutions are abstracted from the hardware components and not dependent on the specific flight stack employed, to allow applying the results to any available autopilot platform with exposed APIs. Two complete vision-based control solutions have been implemented for two different scenarios: keeping the computer driving the computer vision algorithms on board or off-board the vehicle itself during flight. The following chapters detail the hardware, libraries, testing environments, and systems used during the development process and how they can be used to develop new control solutions based on available computer vision mechanisms.

1.3 Objectives

The main objective of this project is to demonstrate the available possibilities to develop control solutions for the PX4 autopilot driven by computer vision mechanisms.

More specifically, it aims to:

- Introduce the software and hardware environment of the Dronecode project and the techniques they have made available.
- Show the minimum requirements needed to develop control software for the platform.
- Suggest viable vision-driven control solutions that use those techniques.
- Present a testing process using available tools that can help ensure safety and reliability for any new solutions developed.
- Build a quadcopter and use it to carry out test flights with the developed solutions.

1.4 Time planning

Write: time planning

1.5 Thesis layout

This sections details the structure of this thesis. The work is composed of five individual chapters that reflect the four distinct phases described in the last section.

- In the first chapter there is a brief introduction to the context in which the project has been developed, as well as the objectives it pursues.
- Chapter 2 presents the technologies and tools employed in this project and the current state-of-the-art of vision-based control solutions for UAVs.
- The third chapter introduces the simulation environments used for development of the solutions throughout the entire project and the architecture of both the hardware used and the software developed.
- Chapter 4 follows along through the process of testing every part of the system incrementally until reaching the final flight tests.
- The last chapter shows the conclusions drawn from the work and presents ideas for future development.

Chapter 2

State of the art

2.1 Literature review

Vision-based control solutions for UAVs on low-cost platforms have gained significant attention recently due to the increasing demand for cost-effective and efficient aerial applications. This literature review summarizes the existing research in this field and highlights the key findings and challenges.

A significant amount of research has focused on developing algorithms for real-time image processing, with a focus on improving the accuracy and robustness of tracking solutions for UAV applications. In [10], a computer vision algorithm for position measurement and velocity estimation using optical flow is proposed for tracking ground-moving targets. In [5], the focus is to solve the problem of tracking and following a generic human target by a drone in a natural, possibly dark scene without relying on color information. In [26], several algorithms are developed to design path-following mechanisms to maintain a constant line of sight with the target. These studies attempt to develop solutions that can be applied to any platform regardless of any preexisting autopilot control in the UAVs. They focus on low-level software implementations of complex control theory topics and advanced mathematics. In contrast, this thesis aims to abstract as much as possible both the control technics and the computer vision mechanisms of detection and tracking to focus on presenting an easy-to-use platform that can employ already developed algorithms and combine them to make robust systems with a lower threshold of expertise.

Some studies have already been centered around developing lower-cost solutions for more accessible platforms. Many have used the Parrot AR.Drone camera-enabled quadcopter that allows controlling through WiFi from an external offboard computer. In [3], [7], [23], and [11], the AR.Drone is used for implementing object tracking and following solutions in different environments and conditions with a higher emphasis on the type of trackers employed to achieve a robust visual following mechanism. In [13], [19], and [6], there is a higher focus on exposing the capabilities of the AR.Drone as a platform to develop custom control solutions utilizing the navigation and control technology and the low-cost sensors already embedded in the vehicle. The main difference between the platform used in the mentioned research and the PX4 platform that has been the target of this thesis is that the AR.Drone is offered as-is, as a concrete low-cost vehicle for which autonomous guidance and control can be developed, while the PX4 platform is a part of an extensive environment that encompasses everything from the minimum essential hardware to the low-level autopilot mechanisms to the high-level control commands and allows complete personalization at each layer of the system.

As the PX4 platform has been available for less than a decade and has only become a widely-recognized standard in the drone industry since 2020, there is still little research on its ecosystem and fewer specific computer-vision projects have been developed. However, some studies do share some of the possibilities that the PX4 software and the Pixhawk flight controllers offer in the field. In [21], aerial images are analyzed in real-time and fed to a

deep-learning architecture to calculate optimal flight paths. In [22], a vision-based precision landing method for quadcopter drones is developed on the Pixhawk flight controller to prevent crashes on landing.

Another vital advantage of the PX4 platform over other available platforms is its compatibility with a wide range of simulators that allow the development of complex control systems in changing environments without the need for expensive, time-consuming, and careful testing of the correct integration of the hardware and software components that real-world flight tests of UAVs entail. Some studies have carried out developments in this area for the ecosystem. In [9], the Gazebo simulator and the PX4 software are used to develop a system for simulating real navigation conditions for obstacle avoidance. In [8], a similar ROS-Gazebo environment serves as the basis for designing fault-tolerant controllers that can recover from rotor failure. In [15], the aim is to integrate a photo-realistic environment simulator with a flight-dynamics simulator as a means to develop full autonomy in the Pixhawk autopilot board. These represent only some of the possible applications of such a complete ecosystem of development solutions.

In conclusion, vision-based control solutions are still a relatively new field in the broader topic of autonomous guidance and navigation for UAVs. Some older low-cost platforms have been more widely employed in research as the basis for developing accessible control systems driven by computer vision. However, for PX4-driven UAVs, there are still many unexplored possibilities when it comes to applying the simulator capabilities of the platform to the development of vision-based control solutions and taking advantage of modern rendering techniques to simulate complex detection and tracking scenarios that reduce the need for difficult real-world flight tests.

2.2 Methodology

This section describes the software programs and libraries employed in this project, as well as the hardware used to carry out flight tests for the developed application.

2.2.1 Software

PX4 autopilot

PX4 [1] is a professional open-source autopilot flight stack developed in C++ by developers from industry and academia, and supported by an active world-wide community, it powers all kinds of vehicles from racing and cargo drones through to ground vehicles and submersibles. The flight stack software runs on a vehicle controller or flight controller hardware. It supports both Ready To Fly vehicles and custom builds made from scratch, as well as many additional kinds of sensors and peripherals, such as distance and obstacle sensors, GPS, camera payloads and onboard computers.

PX4 is a core part of a broader drone platform, the Dronecode Project [2], that includes the QGroundControl ground station, Pixhawk hardware, and MAVSDK for integration with companion computers, cameras and other hardware using the MAVLink protocol. PX4 was initially designed to run on Pixhawk Series controllers, but can now run on Linux computers and other hardware. The software controls the vehicles through flight modes. Flight modes define how the autopilot responds to remote control input, and how it manages vehicle movement during fully autonomous flight. The modes provide different types or levels of autopilot assistance to the user, ranging from automation of common tasks like takeoff and landing, to mechanisms that make it easier to regain level flight or hold the vehicle to a fixed path or position.

MAVLink and MavSDK

MAVLink [3] is a very lightweight messaging protocol for communicating with drones and between onboard drone components. It follows a modern hybrid publish-subscribe and point-to-point design pattern where data streams are published as topics while configuration sub-protocols such as the mission protocol or parameter protocol are sent as point-to-point with retransmission. Messages are defined within XML files. Each XML file defines the message set supported by a particular MAVLink system.

[1] https://px4.io/
[2] https://www.dronecode.org/
[3] https://mavlink.io/en/

MAVSDK [4] is a cross-platform collection of libraries for various programming languages to interface with MAVLink systems such as drones, cameras or ground systems. It is primarily written in C++ with wrappers available for, among others, Swift, Python and Java. The Python wrapper is based on a gRPC (Google Remote Procedure Call) client communicating with the gRPC server written in C++. The libraries provides a simple API for managing one or more vehicles, providing programmatic access to vehicle information and telemetry, and control over missions, movement and other operations. The libraries can be used onboard a drone on a companion computer or on the ground for a ground station or mobile device.

QGroundControl

QGroundControl [5] is an open-source ground control station for the MAVLink protocol that provides flight control and mission planning for any MAVLink enabled drone. It is designed with focus on ease of use for professional users and developers. QGroundControl connects automatically to flight controllers running the PX4 Autopilot, either through cable or wireless connection to the computer running the ground station, as well as to any simulator running the PX4 flight stack.

The software enables setting up the initial configuration of a flight controller and calibrating sensors and other peripherals connected to it, editing and keeping track of modified configuration parameters and sending flight commands to the drone, like arming, take-off and landing. It provides a map interface to keep track of the vehicles GPS location as well as to select target location points for planning flight missions, where the vehicle goes through each planned point at the designated speed and altitude. Figure 2.1 shows the interface of the application on a Windows system.

Unreal Engine

Unreal Engine [6] is a 3D computer graphics creation tool, best known for its game development capabilities. It was first released in 1998 to develop first-person shooters, but its features have expanded over the years and the engine is now used on all kinds of fields like film and television, to create virtual sets, real-time rendering and computer generated animation, and research, especially as a basis for virtual reality tools and developing virtual environments for the design of buildings and vehicles, among others, employing the engine's support for real-time graphics. Figure 2.2 shows the program's interface when a project is loaded into the engine.

[4] https://mavsdk.mavlink.io/main/en/index.html
[5] http://qgroundcontrol.com/
[6] https://www.unrealengine.com/en-US

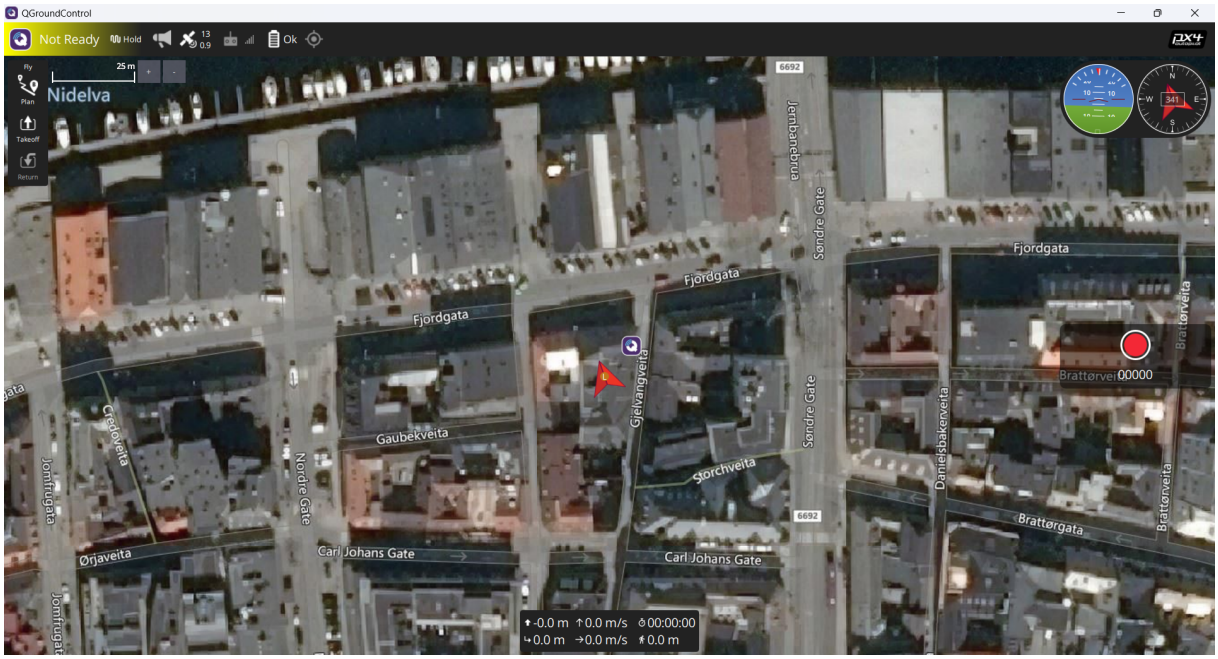

Figure 2.1: Main interface for the QGroundControl program

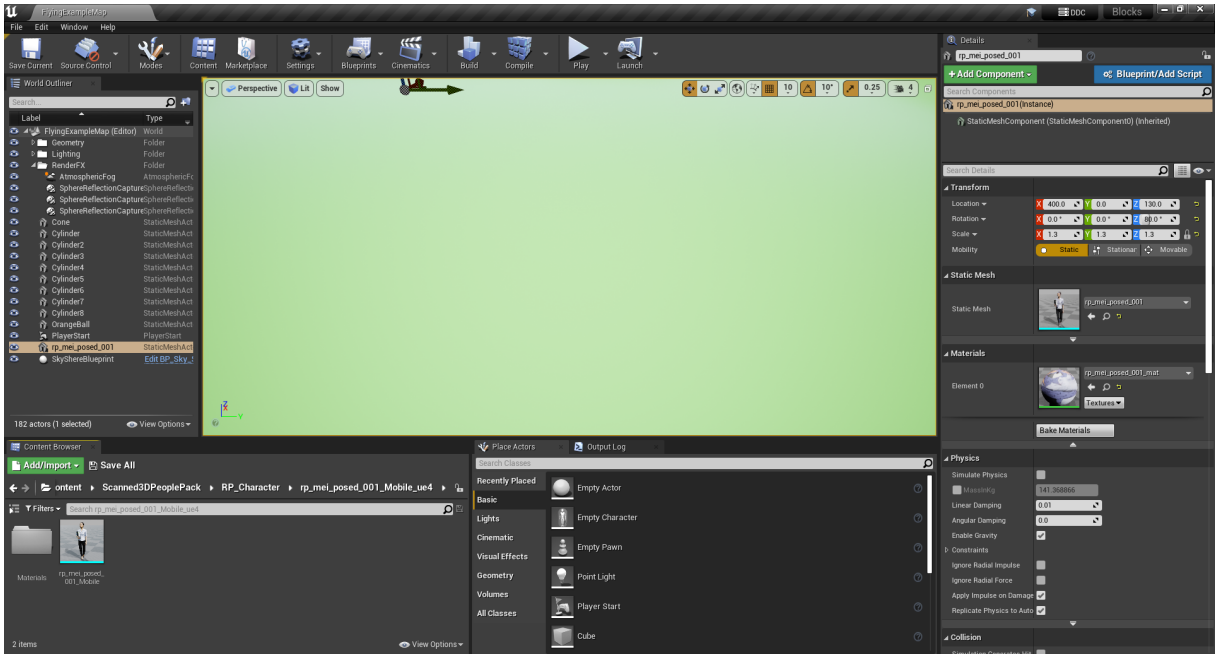

Figure 2.2: Project interface for the Unreal Engine

AirSim

AirSim [7] is a simulator for drones, cars and more, built on Unreal Engine and developed by Microsoft. It is open-source, cross platform, and supports software-in-the-loop (SITL) simulation with popular flight controllers such as PX4 and ArduPilot and hardware-in-the-loop (HITL) with PX4 for physically and visually realistic simulations. It is developed as an Unreal plugin that can simply be dropped into any Unreal environment.

Its goal is to develop a platform for AI research to experiment with deep learning, computer vision and reinforcement learning algorithms for autonomous vehicles. For this purpose, AirSim also exposes APIs to retrieve data and control vehicles in a platform independent way.

MediaPipe

Mediapipe [8] is an open-source project developed by Google that offers cross-platform, customizable machine learning solutions for live and streaming media. It supports End-to-End acceleration with built-in fast ML inference and processing accelerated even on common hardware and a unified solution that works across Android, iOS, desktop/cloud, web and IoT. It offers a framework designed specifically for complex perception pipelines, like real-time perception of human pose, face landmarks and hand tracking that can enable a variety of impactful applications, such as fitness and sport analysis, gesture control and sign language recognition, augmented reality effects and more.

GitHub

GitHub is an online hosting service using the distributed version control system Git for software development. It is currently the largest source code host with over 350 million repositories.

OpenCV

OpenCV is an open-source library for computer vision, machine learning and image processing that counts with over 2000 algorithms. It can be used to retrieve images or videos from cameras, extract data from them and edit them. It is developed in C++ but has

[7] https://microsoft.github.io/AirSim/
[8] https://google.github.io/mediapipe/

Python-wrappers available that take advantage of the general purpose programming language while maintaining the speed of the underlying computationally intensive C++ code. OpenCV-Python employs the Numpy library, which is designed for highly optimized numerical operations with syntax based on the MATLAB style. In Python, all the OpenCV array structures are converted to and from Numpy arrays. This makes it easy to work together with other libraries that use Numpy like Matplotlib for plotting graphs.

2.2.2 Hardware

Pixhawk 4

The Pixhawk 4 is an advanced autopilot module designed and produced by Holybro[9], a UAV parts and kits manufacturer, in collaboration with the Dronecode Project team. It is based on the Pixhawk-project [10] FMUv5 open hardware design, and it is optimized to run PX4 on the NuttX [11] operating system by the Apache Foundation. The Pixhawk 4 has an integrated accelerometer/gyroscope, a magnetometer, and a barometer, which enables it to drive an unmanned vehicle using the PX4 flight stack natively without any other sensors. It includes as well many connector sockets to extend its features with additional sensors, input/output devices, or a companion computer. Figure 2.3 shows the autopilot module with all its connectors and buttons.

Holybro X500

The Holybro X500 [12] is a quadcopter designed by Holybro to use with PX4. It comes as a ready-to-assemble development kit made up of a full carbon-fiber twill frame and the Pixhawk 4 flight controller. The kit includes as well a power management board, four motors, a GPS module, an RC receiver, and a telemetry radio. It has a build time of approximately 3 hours and does not require any specialized tools for the process. Figure 2.4 shows the final result of the building process.

Raspberry Pi 4

The Raspberry Pi [13] is a line of single-board computers that stands out thanks to its affordable price, compact size, and maker-friendly design. Model 4B is an improved version of

[9] https://shop.holybro.com/
[10] https://pixhawk.org/
[11] https://nuttx.apache.org/
[12] https://docs.px4.io/main/en/frames_multicopter/holybro_x500_pixhawk4.html
[13] https://www.raspberrypi.com/products/raspberry-pi-4-model-b/

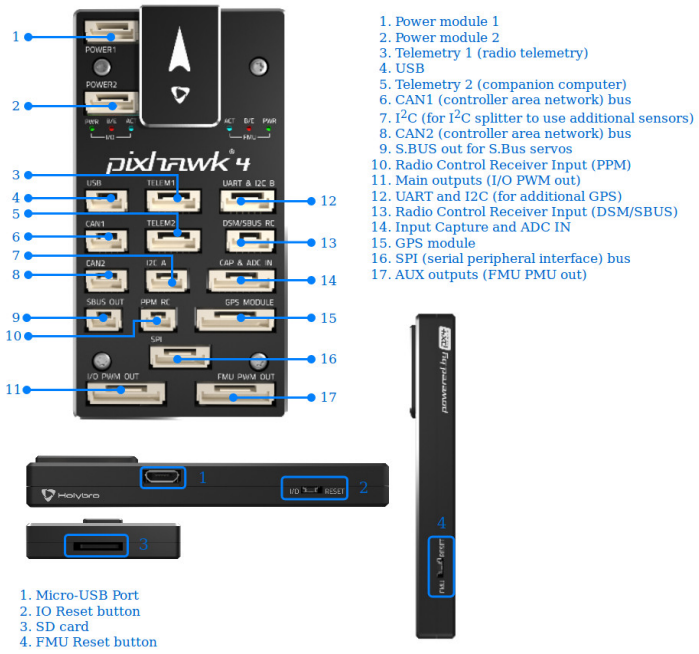

Figure 2.3: Side views and connector map for the Pixhawk 4 autopilot module.

Source: Adapted from *PX4 User Guide* [24].

its predecessors, significantly increasing processing power, enhanced video output, and peripheral connectivity while maintaining the same low price and tiny size offered on past models. This small computer comes as a bare circuit board, without any housing or add-ons, such as a cooling fan or a power button, but it includes USB, HDMI, and Ethernet ports and both Wi-Fi and Bluetooth connectivity, as well as a 40-pin GPIO GPIO header, a row of input/output pins that provides direct access for connecting external devices. The Raspberry Pi runs natively Raspbian OS, a free operating system based on Debian optimized for the Pi hardware, but it is compatible with other standard flavors of Linux.

Figure 2.4: Fully assembled X500 kit.

Source: Adapted from *PX4 User Guide* [24].

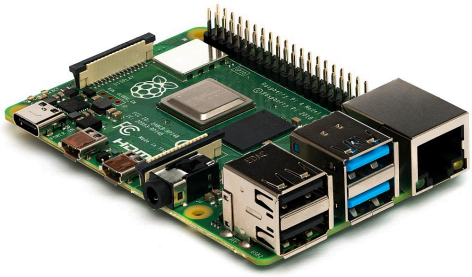

Figure 2.5: Raspberry Pi 4 Model B

Source: Wikimedia Commons [2].

Chapter 3

Design and implementation

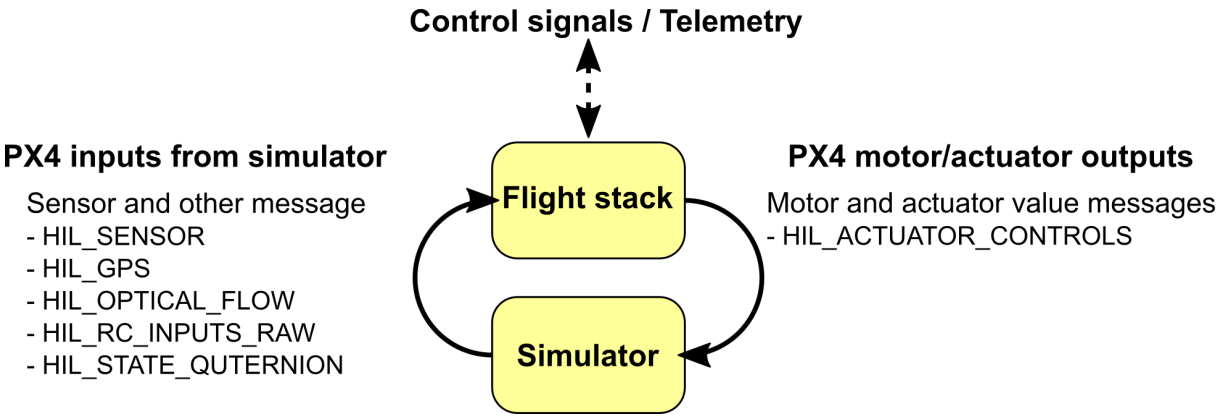

Figure 3.1: Mavlink messages exchanged between the simulator and the flight stack during simulation.

Source: Adapted from *PX4 User Guide* [24].

3.1 Development environment and simulation

During the process of developing the application, it became necessary to be able to continuously deploy and test the latest version without having to depend on flying the physical vehicle but instead relying on the simulation of the system inside the computer that was at the same time running the developed software. This configuration has the twofold advantage of reducing the development time on the one hand, since there is no need to be concerned with the interactions between the different hardware components and the results can be visualized immediately on the computer screen, and on the other hand increasing the safety of the process by only running on the vehicle software that has already been tested to an acceptable point.

Simulators allow PX4 flight code to control a computer-modeled vehicle in a simulated "world" that can be interacted with in the same ways as with a real vehicle, using QGroundControl, an offboard API or a radio controller/gamepad. PX4 supports two different simulation modes: software-in-the-loop (SITL), where the flight stack runs on an external computer, and hardware-in-the-loop (HITL), where it uses a simulation firmware on an actual flight controller board. Communication into and out of the flight stack uses the MAVLink protocol mentioned in section 2.2.1, which allows exchanging of messages defined within XML files between drones, ground control stations, and other MAVLink systems [16]. When the firmware is simulated, a MAVLink server is always started as part of the running software to enable communication with the simulator program and any other offboard entry point that could be present.

In both SITL and HITL modes, the simulation works according to the feedback loop shown in figure 3.1. The simulator generates the input from the sensors based on its internal world representation and sends it through Mavlink messages to the flight stack running

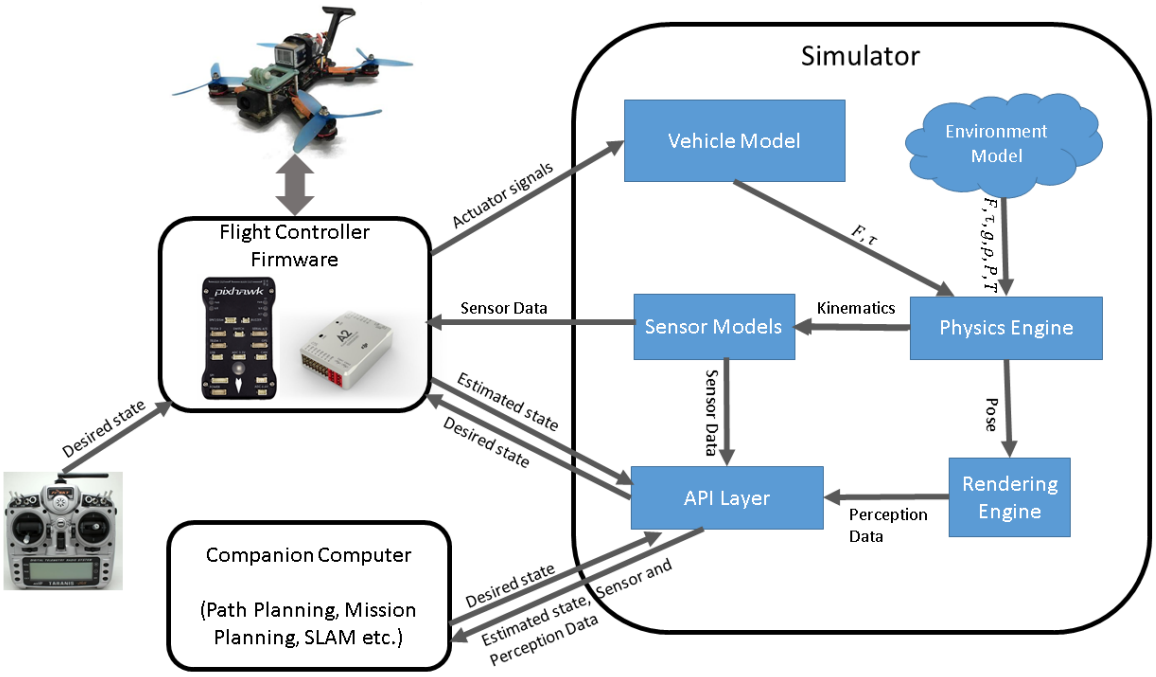

Figure 3.2: High-level overview of how different components interact in the AirSim simulator.

Source: Adapted from *Aerial Informatics and Robotics Platform* [27].

on the same computer using the UDP transport protocol, which in turn generates response actuator controls that are fed back into the simulator in the same way to affect the vehicle's position, velocity, and attitude in the simulated world. Simulated communications employ MAVLink messages specific to the mode in use and are not precisely the same as those used during non-simulated flight.

There are many options for simulators supported by PX4, like Gazebo, a powerful 3D simulation environment for Linux systems that is particularly suited for testing object avoidance and is commonly used with ROS, or AirSim (2.2.1). This more resource-intensive cross-platform simulator leverages the Unreal Engine, typically used for game development and animation, to provide physically and visually realistic simulations. For this project, AirSim was chosen because of previous experience with Unreal Engine as well as for the easy availability of visual packages to test computer vision features and its native support for running on Windows machines, which is the operating system running on the computer where the tests will take place. AirSim offers as well a Python library called `airlib` ([1]) that can be used to retrieve images taken from a simulated camera from the perspective of the drone in the simulation world. This feature will be necessary when testing the person-recognition utilities used in the program.

[1] https://pypi.org/project/airsim/

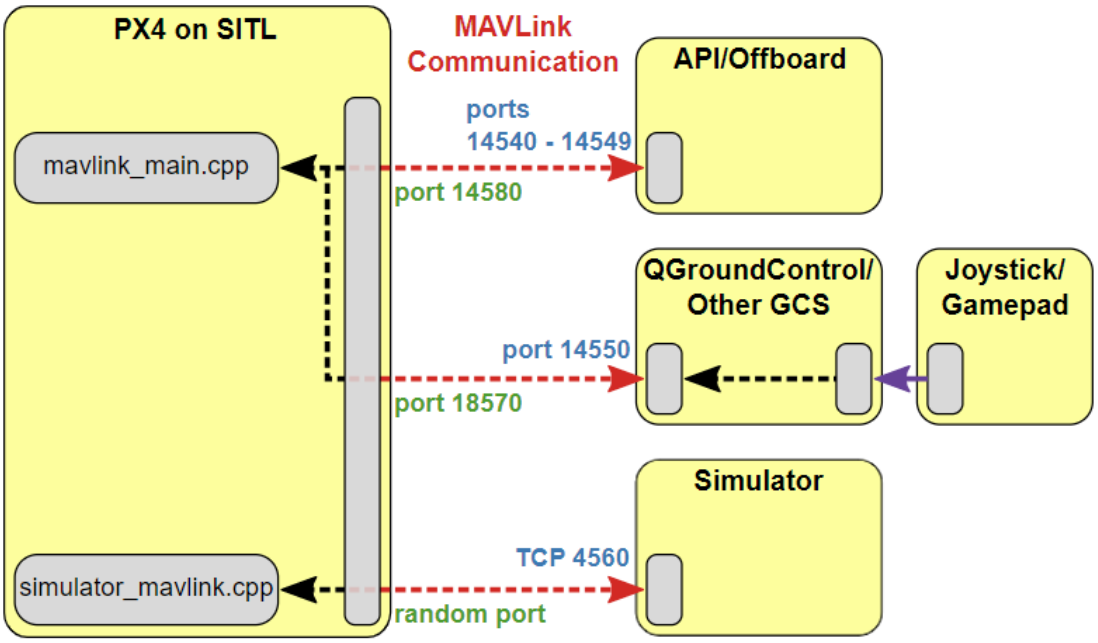

Figure 3.3: Network diagram between the different components that interconnect during software-in-the-loop simulation.

Source: Adapted from *PX4 User Guide* [24].

Polish: export all boards again from Miro without watermarks

A high-level overview of the simulator architecture and the way different components interact with each other can be seen in figure 3.2. The API layer present in the Figure inside the simulator environment refers to AirSim's own airlib library, which exposes with high-level functionality to send control commands to the flight controller directly. However, in order to share the same control code when simulating flight and in real flight without and not depend on the simulator system, the control commands are sent using the official MavSDK API instead, which allows communication of estimated state, desired state and sensor data directly between the flight controller firmware and the companion computer.

In order to run software-in-the-loop simulation, the PX4 firmware needs to be built from the source code on the Linux platform where it is going to run. The build system then sets up all the necessary ports for the Mavlink communication and starts a local instance of the NuttX operating system that runs on the actual flight board. Figure 3.3 shows how the different parts of the system communicate with each other inside a SITL simulation. PX4 uses commonly established UDP ports for MAVLink communication with ground control stations (e.g. QGroundControl), offboard APIs (e.g. MAVSDK, MAVROS) and simulator APIs (e.g. AirSim, Gazebo). External developer application like Dronecontrol use an offboard API, in this case MAVSDK, and therefore listen to PX4's remote UDP

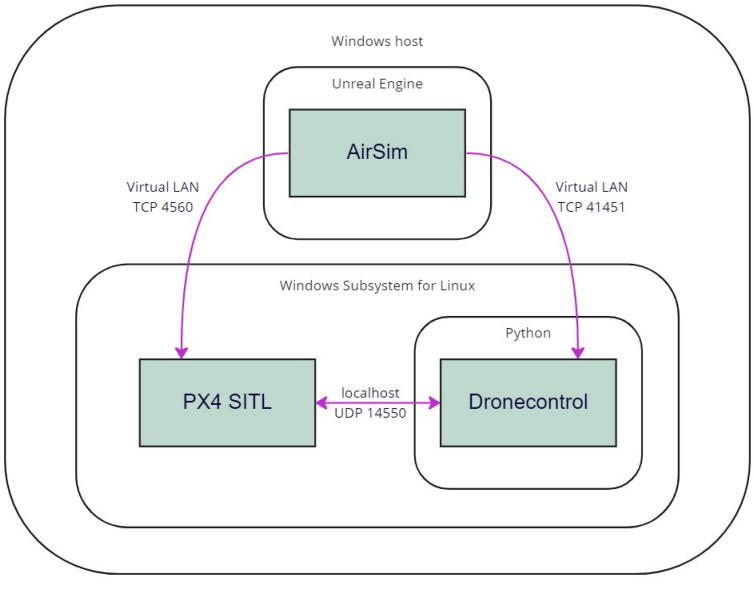

Figure 3.4: Connection diagram of how the three systems interact with each other during SITL simulation.

port 14540. All ports in the range 14540-14549 can be used to connect offboard API, for example in the case of controlling multiple vehicles at the same time. PX4's remote UDP Port 14550 is used for communication with ground control stations, which are expected to listen for connections on this port (QGroundControl listens to this port by default). PX4 uses a simulation-specific module to connect to the simulator's local TCP port 4560. Simulators then exchange information with PX4 using the Simulator MAVLink API shown in Figure 3.1. PX4 on SITL and the simulator can run on either the same computer or different computers on the same network.

Since the purpose of using AirSim as a simulator is to run it on a Windows computer and the PX4 software-in-the-loop stack runs on Linux, it is necessary to run a virtualized Linux OS in parallel on the Windows computer and setup a local network so that the simulator and the flight controller firmware can communicate with each other. The PX4 development team officially supports running the SITL flight stack in Windows through the Windows Subsystem for Linux (WSL2)[2], which allows users to install and run their Ubuntu Development Environment on Windows as if it was running it on a Linux computer. The Windows Subsystem for Linux lets developers run a GNU/Linux environment (including most command-line tools, utilities, and applications) directly on Windows, unmodified, without the overhead of a traditional virtual machine or dualboot setup. The full steps needed for to configure the system are detailed in Section **??**.

The whole set of connections established in the software-in-the-loop simulation is shown

[2] https://docs.microsoft.com/en-us/windows/wsl/about

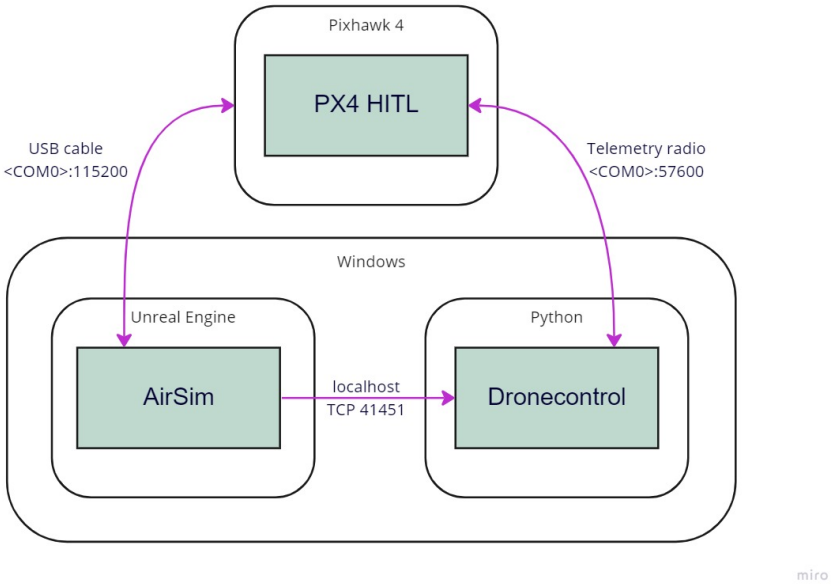

Figure 3.5: Connection diagram of how the three systems interact with each other during HITL simulation.

in Figure 3.4 at the transport layer level. The two systems that run inside the virtualized Linux system through WSL (the simulated flight stack and the dronecontrol program) connect through the localhost network on the UDP port defined by PX4 for Offboard APIs and each of them connects in turn to the AirSim simulator through the virtual Local Area Network established by the Windows Subsystem for Linux to the host Windows computer. The PX4 flight stack on SITL mode connects to the simulator using the TCP port 4560, as defined by PX4 on Figure 3.3, and dronecontrol connects through the AirSim library which uses by default a TCP connection on port 41451.

In the case of hardware-in-the-loop simulation, the main difference with SITL is that the flight stack firmware runs on a physical flight board using a special configuration. In HITL all motors/actuators are blocked, but internal software is fully operational. This configuration adds an additional separated operating system and to make this mode of testing simpler, since the WSL environment is no longer needed to run the flight stack, it is possible to move the execution of the Python module to Windows. This eliminates the need to add further configuration to allow the external flight controller to communicate with the internal WSL network, which is by default only accessible by its Windows host computer. Moreover, now that PX4 runs on a separate piece of hardware, it is necessary to establish two separate physical connections to the Windows computer, so that both the simulator and the Python app can communicate through their own channel to the flight controller, either wired, to the microUSB port or an unused telemetry port on the flight controller, or wireless through a telemetry radio.

Figure 3.5 shows the chosen connections to execute tests in HITL mode. The Windows

machine runs both AirSim and the Python interpreter, which communicate through the `localhost` network using TCP. The board running PX4 connects to the simulator through a USB to microUSB cable, which is setup to work with a baudrate of 115200, and to the developed program through a telemetry radio running at a baudrate of 57600, both attached to USB ports on the Windows computer accessible through their COM address.

AirSim testing environment

Unreal Engine is a complex computer graphics generation program. It works by creating environments where components like 3D models, cameras, and lighting can be added. AirSim is a plugin made for this engine by Microsoft, and although it also has a release for the other main game engine in the market, Unity, it is experimental and limited in features. The documentation contains all the necessary steps to get Unreal Engine and AirSim running on a Windows, Linux, or macOS operating system. However, it works best on Windows [20]. The source code for the AirSim project includes a built-in Unreal environment that can be used to run tests and contains several 3D shapes like block and spheres, as well as a default quadcopter to act as the control vehicle. It is also possible to create custom Unreal environments and run AirSim inside them by adding the built plugin to the project and a custom vehicle.

The environment used in this project for testing the Dronecontrol application is derived from the built-in AirSim environment. It contains the default quadcopter vehicle, which includes several virtual cameras in order to be able to retrieve images from the vehicle's point of view in the simulated world, and a few of the preset blocks with a green color to give a better contrast to the camera. The main addition to the environment is the 3D model of a human figure, to be used for testing the pose detection and tracking mechanisms of the computer vision solution. The model is part of a free asset library of human models made by Renderpeople [25] obtained in the Unreal Marketplace. An image of the testing environment can be seen in figure 3.6.

AirSim is compatible both with SITL and HITL simulation. However, it is necessary to set it up to work with an external PX4 flight controller instead of AirSim's own internal `SimpleFlight`. Appendix A.4 shows all the required settings for configuring these modes in AirSim. To run the simulator in Windows and the flight controller in WSL, the IP of the Windows host in the `vEthernet (WSL)` network needs to be provided in the AirSim settings. This process is detailed further in the AirSim documentation [**airsim-doc-wsl**]. In brief, first the Unreal project with AirSim has to be set into play mode and then the PX4 SITL flight controller built and run to attach to an already running simulator. Inside the project in WSL, the flight controller can be run for AirSim by using the provided shortcut script [3]:

[3] https://github.com/l-gonz/tfg-giaa-dronecontrol/blob/main/simulator.sh

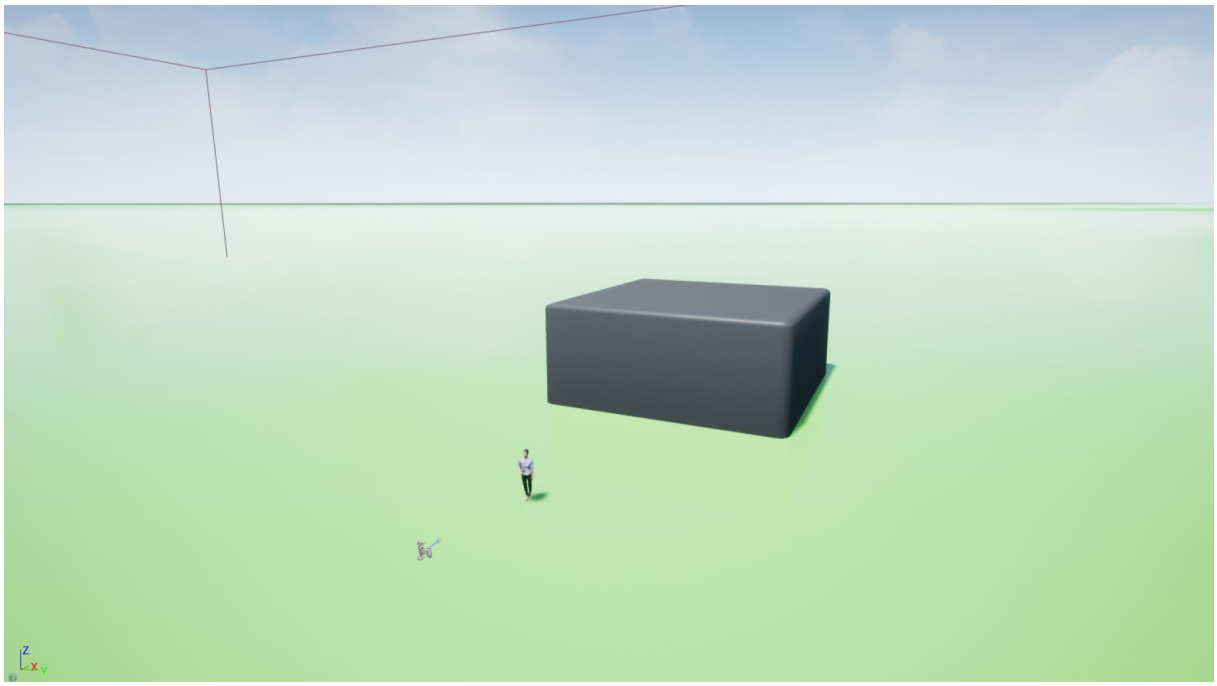

Figure 3.6: Screenshot from the Unreal Engine environment used for testing the computer vision solutions.

```
sh simulator.sh --airsim
```

Once both the simulator and the flight controller are connected, an RC controller or QGroundControl can be used to control the vehicle, and other offboard applications like Dronecontrol can be attached to send any desired MAVLink commands.

For HITL, the `UseSerial` setting should be set to true in the AirSim configuration and the Pixhawk board connected to an USB port in computer, as well as HITL mode enabled in the board from QGroundControl. Then, the simulator will attach automatically to the board after starting play mode in Unreal. Once the simulation has started, there is no noticeable change between the simulated flight controller in the computer (SITL mode) and the one running in the physical board (HITL mode).

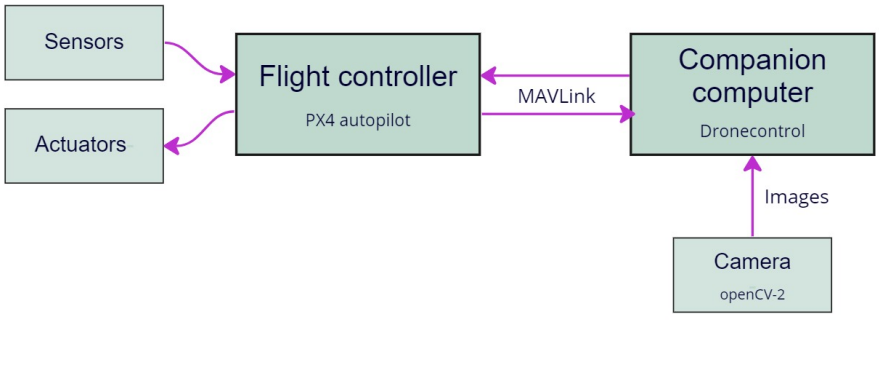

Figure 3.7: Top level diagram of the hardware/software interactions

3.2 System architecture

3.2.1 Top level

The purpose of the Dronecontrol application is to be able to direct the movement of a Unmanned Aerial Vehicle (UAV) through the analysis of the images taken by a camera. Since the processing power needed to work with the images recorded is superior to that offered by the autopilot flight controller it becomes necessary the use of an additional companion computer that will control the camera and employ machine learning to extract useful features from the images, as well as transform those features into movement directives for the vehicle.

A top level diagram of the individual parts that comprise the system is shown in Figure 3.7. The main elements are the flight controller, that will run the PX4 autopilot 2.2.1, the companion computer, that will run the developed application, and the camera, which provides the images. The flight controller interfaces directly with the companion computer using the MAVlink protocol described in Section 2.2.1, either through a wireless radio link or a cabled serial connection between the two. The camera is connected to the companion computer through a cable into an USB port on the computer. Typically, the type of connection between the flight controller and the computer depends on the desired setup for the system so in the case where the camera, and therefore the companion computer, flies onboard the vehicle it is most convenient to use a direct wire connection between the two, as it provides a faster and more stable link. This onboard configuration is further detailed in Section 3.2.2. On the other hand, in the case where the companion computer will be acting more like a ground station on an offboard configuration it becomes strictly necessary to communicate with the flight controller through a wireless connection. For this purpose, a pair of telemetry radios provided with the Development Kit of the Holybro X500 (2.2.2)

are used. The complete setup requiered for this configuration is described in Section 3.2.3.

In this project, the flight controller is driven by the PX4 software (2.2.1) and the hardware employed is optimized for this flight stack. PX4 uses sensors to determine the vehicle state, which is needed for stabilization and to enable autonomous control. It minimally requires a gyroscope, accelerometer, magnetometer (compass) and barometer. A GPS or other positioning system is needed to enable all automatic flight modes, and some assisted ones. PX4 uses outputs to control motor speed, flight surfaces like ailerons and flaps, camera triggers, parachutes, grippers, and many other types of payloads. Many PX4 drones use brushless motors that are driven by the flight controller via an Electronic Speed Controller (ESC). The ESC converts a signal from the flight controller to an appropriate level of power delivered to the motor. PX4 drones are mostly commonly powered from Lithium-Polymer (LiPo) batteries. The battery is typically connected to the system using a Power Module or Power Management Board, which provide separate power for the flight controller and to the ESCs for the motors. A Radio Control (RC) system is used to manually control the vehicle. It consists of a remote control unit that uses a transmitter to communicate stick/control positions with a receiver based on the vehicle. Some RC systems can additionally receive telemetry information back from the autopilot. Telemetry Radios can provide a wireless MAVLink connection between a ground control station and a vehicle running PX4. This makes it possible to tune parameters while a vehicle is in flight, inspect telemetry in real-time, change a mission on the fly, etc.

On an actual UAV, the PX4 software runs on a dedicated piece of hardware like the Pixhawk 4 flight controller described in Section 2.2.2 that includes all the minimal required sensors for flight as well as interfaces to connect additional actuators and I/O systems (RC, telemetry radio, etc). However, it is also possible to simulate this hardware on a standard Linux system by building the PX4 source code on a computer with this operating system. This process is described in the development environment section (3.1).

The Dronecontrol application that runs on the companion computer has been developed using the Python programming language [4]. It offers good advantages for a project of this characteristics because of its high-level, easy-to-use syntax, that usually results in a smaller code base than other comparable languages for small projects, its versatility and support for object-oriented programming. Most importantly, Python is widely used and its official package manager `pip` greatly simplifies the use of external libraries and which gathers in its package index [5] thousands of standard utilities, including many machine learning and image processing projects and all the required libraries for interacting with PX4 through the MAVLink protocol (MavSDK). As it is an interpreted language, it can run easily in any system with Python installed without the need to compile separate binaries for different operating systems.

[4] https://www.python.org/
[5] https://pypi.org/

The next sections explore deeper into the differences between the two configurations mentioned before: offboard computer (or ground station) and onboard computer.

3.2.2 Offboard computer configuration

The offboard configuration allows the flight controller to communicate and receive orders from a companion computer that is not physically connected to its hardware but that can instead stay on ground while the vehicle flies. This has the advantage that it permits a simpler configuration, without having to be concerned with low-level hardware interactions between the two systems or powering of the companion computer while in flight, as well as allowing the use of a more powerful computer for image processing. However, it also requires that the camera stays connected to computer on the ground so it cannot use images from the perspective of the drone in flight which limits the real-world applications of the system. Other configurations involving a direct connection from a camera to the flight controller and the transmission of its images wirelessly to the companion computer through mavlink for processing can be feasible with the current technology but fall out of the scope of this project.

The wireless link is established in this instance through a pair of telemetry radios that connect to a telemetry port on the flight controller and to a USB port in the companion computer, respectively. Since the Pixhawk 4 is configured by default to used its `TELEM1` port for this purpose, no additional configuration is needed when using that port. In the companion computer, applications like the QGRoundControl [6] ground station software which is part of the Dronecode Project are able to detect automatically a telemetry radio inserted into any of the USB ports of the host computer. Additionally, other applications using the MavSDK (2.2.1) library can establish connection specifying the baudrate and the USB serial port address, usually something similar to `/dev/ttyUSB0` on Linux and `COM1` on Windows.

The radio used for the physical tests in this project is the Holybro SiK Telemetry Radio [7]. It is a small, light and inexpensive open source radio platform that typically allows ranges of better than 300m "out of the box" (the range can be extended to several kilometres with the use of a patch antenna on the ground). The radios are offered either as 915Mhz (Europe) or 433Mhz (US) so they can be used in different regions and comply with the regulations for frequency, hopping channels and power levels. They offer 2-way full-duplex communication through an adaptive TDM UART interface and their antenna allows for an adjustable 100-mW-maximum output power and -117 dBm receive sensitivity. The link is established by default with a baudrate of 57600 (max bits per second on a serial channel) and it can provide air data rates of up to 250 kbps.

[6] http://qgroundcontrol.com/
[7] http://www.holybro.com/product/transceiver-telemetry-radio-v3/

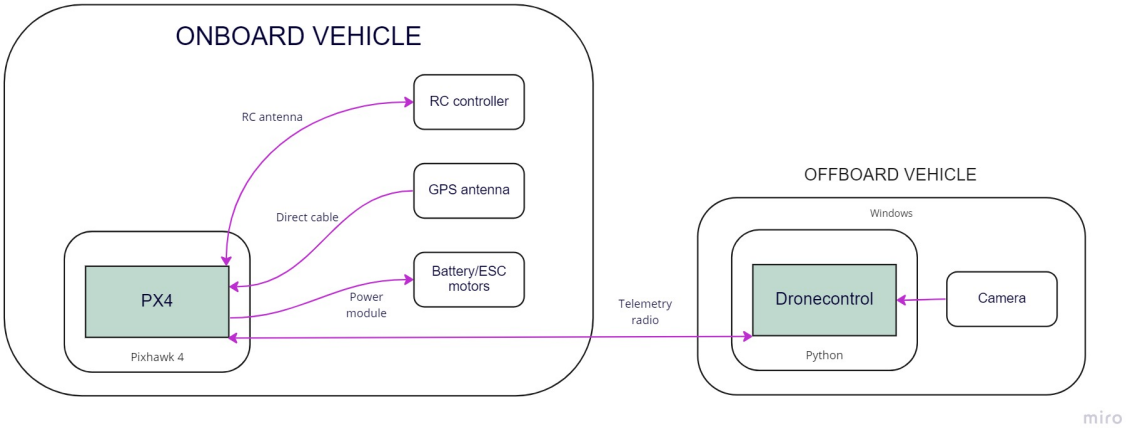

Figure 3.8: Offboard configuration connections

Figure 3.8 shows a summary of all the connections between the PX4 software, the Dronecontrol application, their hardware platforms, and their respective peripherals both onboard the vehicle and at the ground station for the offboard computer configuration setup.

3.2.3 Onboard computer configuration

The second way of configuring the interaction between the flight controller and the companion computer consists of integrating both together on board the UAV. In this case, the connection is done through a direct cable between the serial port in the flight controller and a USB port in the companion computer. The camera will then be connected via cable as well to the companion computer and oriented in the vehicle in a way that allows for the best possible perspective during flight. This configuration makes it possible to develop new control solutions based on images taken directly from the vehicle that reflect the trajectory that it follows. Therefore, it becomes possible to adjust the control loop based on previous reactions of the vehicle to commands and maintain a feedback loop for more stable guidance.

Since the computer running the visual processing algorithm now has to fly on board the vehicle, it becomes especially important to make a good choice when selecting hardware. To be able to take into the air, the computer has to be light enough that its weight can be lifted by the propellers while maintaining adequate battery autonomy, but also powerful enough that the processor can handle the computer vision algorithms required to extract the necessary features from the images taken from the onboard camera that are to be feed to the control loop.

The Raspberry Pi 4 model chosen for this project and shown in Figure 3.9 is one of the

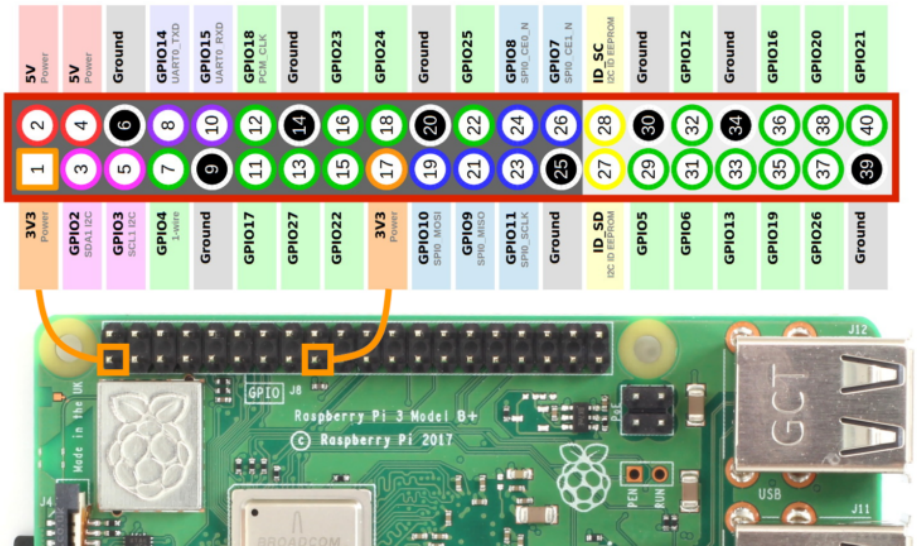

Figure 3.9: The Raspberry Pi 4 microcomputer, with its 40-pin GPIO header marked in red, and its pinout.

Source: Adapted from *Raspberry Pi GPIO Header with Photo* [12]

most popular small computers available in the market at the time, and it is widely used in all kinds of robotics projects both for education and hobbyists. One of the most essential advantages of using such a platform is the easy access to a great number of manuals, guides, and other support available online. In addition, the Raspberry's officially supported operating system, called Raspberry Pi OS, is a Debian-based version of Unix optimized for its ARM microcontroller, simplifying the process of moving from an Ubuntu test environment into actual flight experiments. Since this computer is designed to be easy to integrate with hardware projects it includes a 40-pin GPIO header (marked in red in Figure 3.9) that can be programmed for connecting to any number of external devices.

The Raspberry Pi is powered by a 5V input that can be provided either from its USB-C port or through one of two pins in the header dedicated to this (marked as "5v Power" on figure 3.9. In the case of the particular vehicle build used in this project, the power management board supplying the energy (the Holybro PM07 [8]) also provides 5V to the flight controller, as well as powering the ESCs to the motors. It counts with two power outputs: one of them connected to the flight controller's `POWER1` port and another one that remains unused. A first attempt at supplying current to the Raspberry Pi was tested initially with a direct connection between the second, free output on the power module and the powering pins on the GPIO header with a custom connector. However, the power supply ended up being too unstable for the Pi board, resulting in frequent dips in the supplied current that would affect the processing capabilities of the companion computer. The solution was to

[8] http://www.holybro.com/product/pixhawk-4-power-module-pm07/

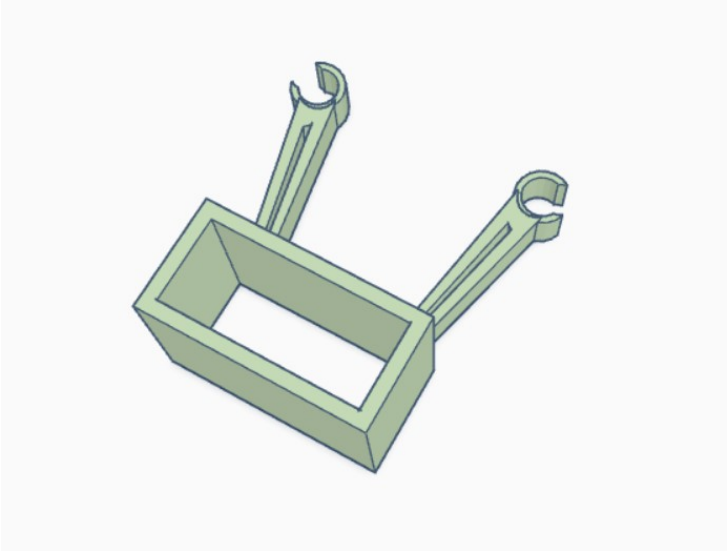

Figure 3.10: 3D model for the camera support designed for the Holybro X500 frame.

add an additional, secondary battery to the build that provides power through an USB cable. This configuration allows the Raspberry to receive power by its default way, through the regulated USB-C port. The disadvantage is that it add one more piece of equipment of substantial weight that needs to be secured to the vehicle's frame and carried into the air while in flight.

In regards to the camera that will fly onboard the vehicle, there are many possibilities to chose from. The most important characteristics that should be looked for are a small weight and simple plug-and-play interaction with the onboard computer. The camera used for the tests carried out and detailed in section 4 is a Logitech C920 1080p webcam [9]. Since the frame of the Holybro X500 is not prepared by default to include an onboard camera, a custom support has been designed and 3D-printed from PLA plastic to be able to hang the camera from the central rods on the underside of the vehicle frame and ensure that it is attached securely during flight. The 3D model of the custom support can be seen in figure 3.10 and the print-ready file can be found in the project repository in GitHub [10].

The second wired connection that needs to be established for this configuration is between the flight controller and the companion computer so the Mavlink messages can be exchanged. As it is desirable to be able to maintain a wireless link to the vehicle even while it is being controlled by the onboard computer, the telemetry radio is kept connected to the `TELEM1` port of the flight controller and the companion computer is wired to the `TELEM2` port. This port is not configured to be used by default so it is necessary to modify the configuration of the Pixhawk board either through QGroundControl or the PX4 console. The required parameter to change in the board is mainly the `MAV_1_CONFIG`, which configures the serial port on which to run a second instance of MAVLink (primary instance

[9] https://www.logitech.com/es-es/products/webcams/c920-pro-hd-webcam.960-001055.html
[10] https://github.com/l-gonz/tfg-giaa-dronecontrol/blob/main/data/camera-holder.stl

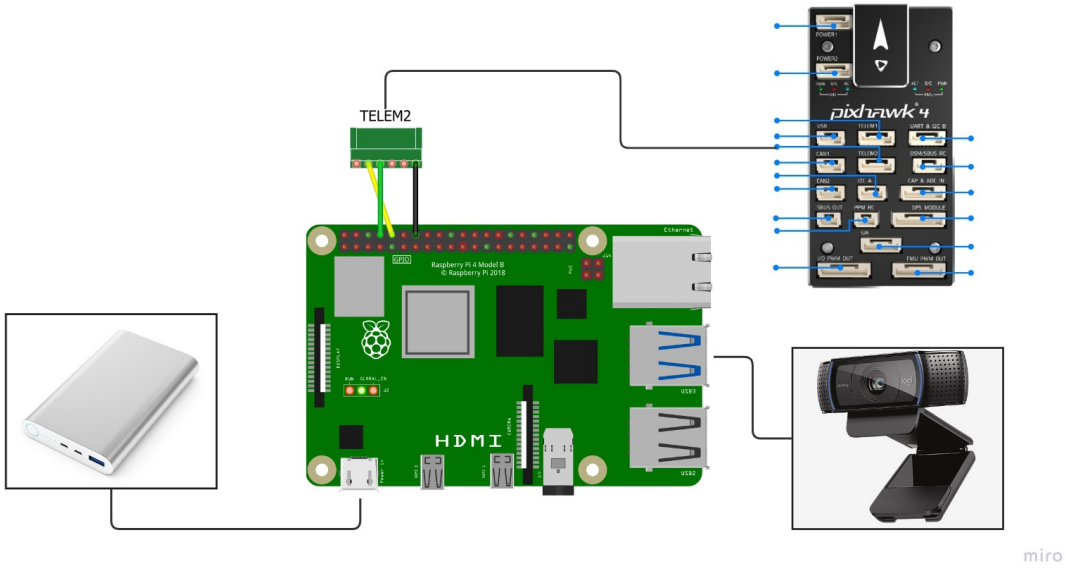

Figure 3.11: A diagram of the wired connections from the Raspberry Pi 4 to the secondary battery and the flight controller (`TELEM2`).

is configured with `MAV_0_CONFIG`), and defaults to 0 (disabled) and should be set to 102 for TELEM 2. This MAVLink instance is set to Onboard mode by default, which is the appropriate mode for communicating with an offboard computer, instead of the Normal mode running on the primary MAVLink instance through `TELEM1` to communicate with QGroundControl. Another parameter to take into account is the `SER_TEL2_BAUD`, which regulates the baud rate of the `TELEM2` port. The default rate is 921600, and it needs to be used when establishing connection in the Dronecontrol application through the MAVSDK library. PX4 provides a complete overview of all the available parameters for the board configuration in their documentation [28].

The other end of the connector has three female Dupont wires that go into the TX/RX UART pins of the Raspberry Pi, according to mapping table 3.1 between the 6 pins in the telemetry connection of the Pixhawk board and the corresponding GPIO pins in the Raspberry Pi header [14] [29]. A diagram of all the connections to the companion computer can be seen in figure 3.11.

Compared to the default baudrate of 57600 on the telemetry radio link established in the previous section, the wired serial connection works at a baudrate of 921600, which means that data can be transferred up to 16 times faster through this link. However, the main limitation on the speed of the program comes from the feature detection process on images, so a faster link rate will not necessarily mean any increase in the overall performance. In section 4.3.2, the behavior of different combinations of hardware is measured further to analyze any challenges to the program's performance.

TELEM2		**GPIO header**	
Pin #	*Description*	*Description*	*Pin #*
1	VCC, +5V		
2	TX (out), +3.3V	GPIO15 (RXD0, UART)	10
3	RX (in), +3.3V	GPIO14 (TXD0, UART)	8
4	CTS (in), +3.3V		
5	RTS (in), +3.3V		
6	GND	GND	6

Table 3.1: Mapping between the `TELEM2` port in the Pixhawk 4 board and the Rapberry Pi's GPIO header.

The offboard configuration allowed the supervision of the output from the program while the vehicle was flying since the computer stayed stationary on the ground. However, in this configuration, it is not feasible to have a screen connected directly to the companion computer. To fix this situation and be able to monitor during flight, as well as being able to give input directly to the program, it is possible to make use of the WiFi receptor of the Raspberry Pi to configure a remote desktop and connect to it through another computer serving as a ground station; Then the camera output and image recognition can be seen in real-time.

Figure 3.12 shows a summary of all the connections present in the onboard configuration between the three pieces of software that interact together: PX4, Dronecontrol and QGroundControl, with their respective hardware platforms and the attached peripherals.

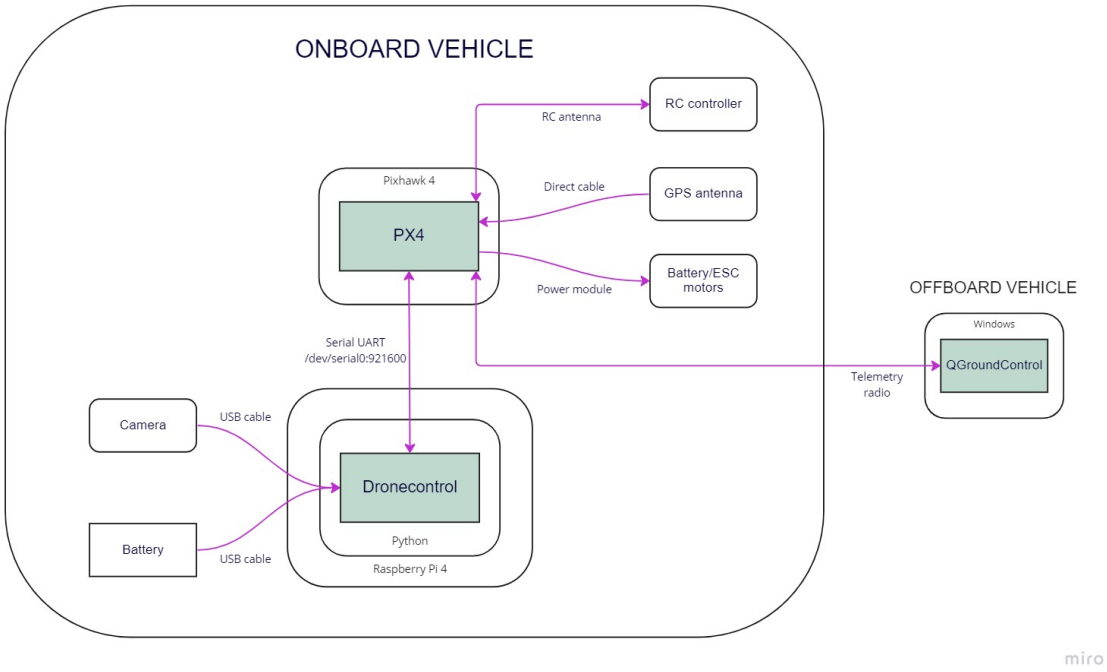

Figure 3.12: Onboard configuration connections

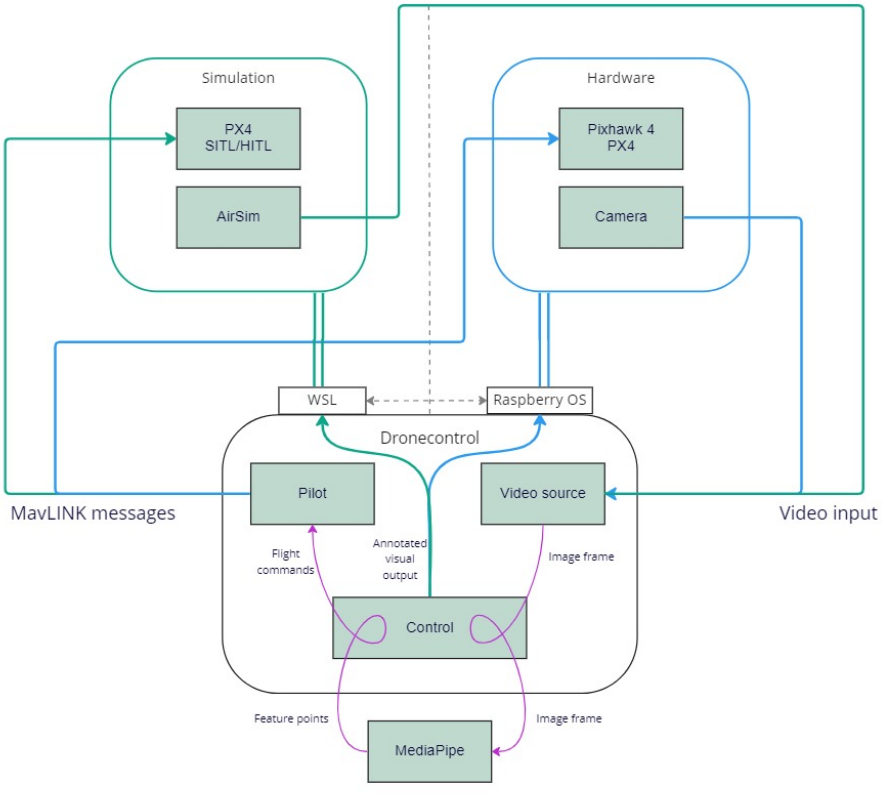

Figure 3.13: Structure of the Dronecontrol application and its interactions with the necessary additional software for running in a simulation (green) or in an actual vehicle (blue).

3.3 Software architecture

Figure 3.13 shows the main modules of the designed software and how it interacts with the external libraries. The application consists of three basic parts: the pilot module, in charge of sending instructions to the flight controller and receiving back information on position and state through the `mavsdk` library, a video source module that handles the retrieval of images from different sources and the necessary processing for image analysis, and a control module that directs the interaction between the other two to transform the pixel information first into position points through the `mediapipe` library and then into instructions for the pilot. The upper part of the diagram in figure 3.13 shows the flow of information between the Dronecontrol application and the external systems, with green lines representing its path in a simulated workflow and blue ones indicating the alternative path for the information in a system with actual quadcopter hardware. Purple arrows show the input/output of each module within the developed application and how they interconnect with each other. Other smaller utilities have also been developed to help test how the systems interact with each other and calibrate different parts of the control behavior. These are described in sections 3.3.3 and 3.5.1. A user manual with all the options available in the application can be found in Appendix A.6.

3.3.1 Pilot module

The purpose of the pilot module is to provide access to the rest of the application to send and receive messages from the PX4 controller through the MavSDK library. This library provides a simple asynchronous API for managing one or more vehicles, providing programmatic access to vehicle information and telemetry, and control over missions, movement and other operations. MavSDK utilizes the python standard library *asyncio* to be able to run coroutines in parallel while waiting for the messages provided through the *MAVLink* communication. Therefore all calls to the library have to be written as async functions that await the result of one or more polls to the flight stack.

`asyncio` provides support for writing concurrent code using the `async/await` syntax. It is used as a foundation for multiple Python asynchronous frameworks that provide high-performance network and web-servers, database connection libraries, distributed task queues, etc; and provides a set of high-level APIs to run Python coroutines concurrently and have full control over their execution. The pilot module integrates `mavsdk` and `asyncio` and provides a queue for the control module to send actions to be executed in the vehicle one after another.

Listing 3.1 shows how to establish a connection to a PX4 vehicle through its physical (serial) or virtual (UDP) address and poll for internal information from the flight controller to decide when the system is ready to receive instructions. The mavsdk library exposes telemetry and other state information through asynchronous generators, which are defined in python as a convenient way to make asynchronous data producers and accessed with the `async for` syntax.

Many of basic operations that can be executed in the flight controller are implemented in the pilot module with error handling and safety checks, like takeoff, landing, return home, or manipulating the vehicle flying velocity directly by providing speeds in body coordinates. These actions can be executed directly or added to a queue that runs in a loop executing them in the order they are added, waiting until the previous action has finished and the vehicle is in the desired state before starting the next. The loop that runs this queue can be seen in Listing 3.2. There is a maximum time of 10 seconds that each action can use to run The loop stops when the asynchronous task it runs on is canceled with `task.cancel()`, which raises a `CancelledError` exception in the parallel execution.

Polish: consider removing code or exchanging for diagrams

```
async def connect(self):
    """Connect to mavsdk server.
       Raises a TimeoutError if it is not possible to establish connection.
    """

    if self.serial:
        address = f"serial:///{self.serial}"
    else:
        address = f"udp://{self.ip if self.ip else ''}:{self.port}"
    self.log.info("Waiting for drone to connect on address " + address)
    await asyncio.wait_for(self.mav.connect(system_address=address),
    ↪  timeout=self.TIMEOUT)

    async for state in self.mav.core.connection_state():
        if state.is_connected:
            break

    # Wait for drone to have a global position estimate
    async for health in self.mav.telemetry.health():
        if health.is_global_position_ok:
            break

    self.log.info("System ready")
    self.is_ready = True
```

Listing 3.1: Example of how the communication to the flight stack is established through asyncio and the mavsdk library

3.3.2 Video source module

The objective of the video source module is to provide a collection of classes to retrieve images from different sources, in a way that they can be exchanged for one another without affecting the rest of the application to facilitate testing and be adaptable to running in different environments. There are three classes of video sources implemented: file, simulator, and camera, which inherit from the same `VideoSource` base class as shown in figure 3.14.

The `FileSource` class is able to open a video file stored in the companion computer and provides images taken frame by frame from it until the video ends. This allows the program to replay the image detection algorithms on videos previously captured by the camera tool exposed in section **??**. The `CameraSource` class can access a physical camera attached to the computer running the application via USB and provide the frames captured in real-time. Both the file and camera sources employ OpenCV's video capture utilities to take care of the file handling and the camera driver management capabilities respectively.

The simulator source uses AirSim's Python library to communicate with the simulator and retrieve images from a simulated camera attached to the 3D model of the vehicle in Unreal Engine. It connects automatically through localhost, but it can also be provided

```
async def run_queue(self):
    """
    Run the queue loop.

    Queued actions will be awaited one at a time
    until they are finished.
    The loop will sleep if the queue is empty.
    """
    try:
        while True:
            if len(self.actions) > 0:
                action = self.actions.pop(0)
                self.log.info("Execute action: %s", action.func.__name__)
                try:
                    await asyncio.wait_for(action.func(self, **action.args), timeout=10)
                except asyncio.exceptions.TimeoutError:
                    self.log.warning(f"Time out waiting for {action.func.__name__}")
            else:
                await asyncio.sleep(self.WAIT_TIME)
    except asyncio.exceptions.CancelledError:
        self.log.warning("System stop")
```

Listing 3.2: Loop where the action queue runs on the pilot module. Each action is awaited until it finishes or the timeout time runs out.

with an IP to establish connection to the simulator running on a different computer on the local network, for example when the program runs inside WSL and the simulator runs on its host computer.

3.3.3 Vision control module

The control module contains the main logic of the application and is in charge of converting the raw images obtained from the video source into commands for the pilot module.

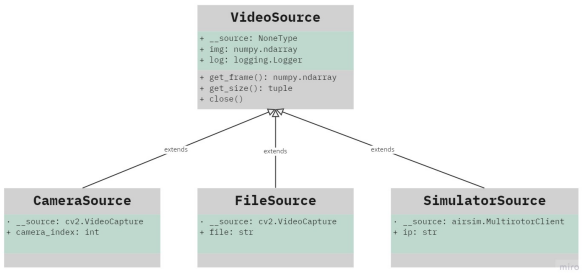

Figure 3.14: Diagram of inheritance on the video source classes available to retrieve image data.

Two different types of control have been implemented. The first one is a proof-of-concept control solution, described in section 3.4, that runs in offboard mode (see section 3.2.2) and translates some predefined hand gestures into simple commands for the aerial vehicle, of which the main purpose is to be able to test the interaction between all the components of the system in a more easily controlled environment, since it uses the simpler configuration of situating the computer with the controller outside of the vehicle. The second control system consists of a follow solution more applicable to real-life scenarios where the control and the camera is onboard the vehicle and the presence of a person is detected in the images obtained from the perspective of the drone in order to be able to give the flight controller velocity commands to follow said person and maintain it centered in its view.

The process followed in both solutions consists roughly of the same two parts. First the image is sent to the computer vision and machine learning third-party library that extracts the required features from the image in the form of 2D coordinates. Afterwards a series of calculations depending on the particular solution are applied to these coordinates to decide which commands are sent to the pilot module. The third-party library used for computer vision in the program is the mediapipe library described in Section 2.2.1, which offers cross-platform, customizable ML solutions for live and streaming media, specifically its hand and pose detection solutions.

To engage the module in direct control of the vehicle's velocity it is necessary to use a special flight mode defined by PX4 for this purpose, called Offboard Mode [11] (not to be confused with the offboard configuration described in section 3.2.2). Offboard mode is primarily used for controlling vehicle movement and attitude, and supports only a very limited set of MAVLink messages. This mode requires position or pose/attitude information to be available to the flight controller, e.g. GPS. In it, the vehicle obeys a position, velocity or attitude setpoint provided over MAVLink by a MAVLink API (i.e. MAVSDK) running on a companion computer and usually connected via serial cable or wifi. A stream of setpoint commands must be received by the vehicle at a rate higher than 2Hz prior to engaging the mode and in order to remain in it. If the message rate falls below 2Hz or the connection is lost the vehicle will stop and, after a timeout, the vehicle will attempt to land or perform some other failsafe action according to the parameters configured. In order to hold position while in this mode, the vehicle must receive a stream of setpoints for the current position.

Sections 3.4 and 3.5 offer a more complete explanation of the control module used by the two different solutions developed.

[11] https://docs.px4.io/main/en/flight_modes/offboard.html#offboard-mode

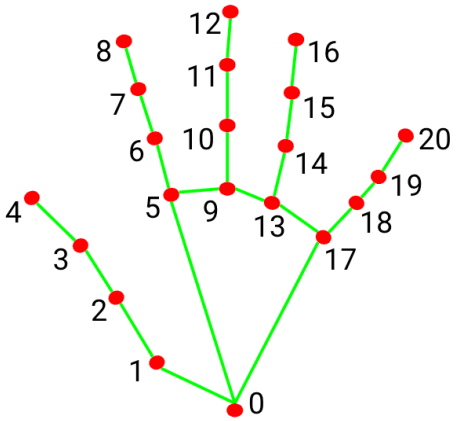

0. WRIST
1. THUMB_CMC
2. THUMB_MCP
3. THUMB_IP
4. THUMB_TIP
5. INDEX_FINGER_MCP
6. INDEX_FINGER_PIP
7. INDEX_FINGER_DIP
8. INDEX_FINGER_TIP
9. MIDDLE_FINGER_MCP
10. MIDDLE_FINGER_PIP
11. MIDDLE_FINGER_DIP
12. MIDDLE_FINGER_TIP
13. RING_FINGER_MCP
14. RING_FINGER_PIP
15. RING_FINGER_DIP
16. RING_FINGER_TIP
17. PINKY_MCP
18. PINKY_PIP
19. PINKY_DIP
20. PINKY_TIP

Figure 3.15: Landmarks extracted from detected hands by the MediaPipe hand solution.

Source: Adapted from *Hands - mediapipe* [17].

Camera-testing tool

Several additional utilities have been added to the dronecontrol program to facilitate the development and testing process of the two main control solutions. The first tool is accessed through the command `dronecontrol tools test-camera` and can be used for testing the connection between the computer, the flight stack and the camera without using any self-guided control mechanism, as well as evaluating the performance of the MediaPipe hand and pose machine learning solution on real time images. It is also possible to take images and record video from the live camera feed for later analysis. Through the command-line options, the test tool can be configured to use any of the three available video sources: camera, simulator or a video file recorded by using the tool itself, to connect to an optional hardware or simulated PX4 flight controller by specifying a connection string or IP, respectively, to run either in a host computer or a WSL subsystem, and to process incoming images with the hand or pose recognition software. While the tool is running, the keyboard can be used to send basic commands to a connected vehicle like takeoff, landing or moving along any of its three axis. A full breakdown of all the tool's options can be found in Appendix A.6.

3.4 Proof of concept: hand-gesture solution

The main purpose of this solution is to test that the flow of the application works as expected, both in simulation and in real flight, and that all the systems are capable of establishing the required connections with each other. For that reason it is designed to be able to be run in real flight with the minimal setup of a built drone with its default components and any computer with a camera.

Figure 3.16: Vectors extracted from the detected features to calculate the relative positions of the individual fingers

This control module runs on a loop that continuously polls for a new frame from the chosen video source and feeds it to the hand detection functionality from MediaPipe [31]. If a hand is detected in the images, 2D coordinates are extracted according to the map shown in figure 3.15. These landmarks are then converted into different discrete gestures like open palm, closed fist or an specific finger pointing different directions. When a new gesture is detected, the command assigned to it is queued to the pilot module and executed as soon as the previous commands end their execution.

The conversion between landmarks and gestures is performed by drawing vectors from the base of each of the fingers to their tips as well as from the base of the hand (wrist feature) to the base of the fingers and using the dot product vector operation to calculate the relative angles between each finger and the base of the hand, as shown in figure 3.16. By comparing the calculated angles to a threshold, it is possible to detect whether each individual finger is extended or folded, as well as the general direction it is pointing towards. The open hand gesture, for example, can then be defined as all five fingers extended, that is, all five vectors defined by the fingers sharing the same approximate angle with the vector from the base of the hand to that finger.

Figure 3.16: hand with arrow vectors between pertinent features and angles origins shown

The full list of gestures detected by the program by calculating these angles is shown in figure 3.17 and is as follows:

- No hand: happens when no landmarks are able to be extracted from the image. As a safety feature, in this case, the vehicle stops whichever previous commands it had in its queue and goes into hold flight mode, where it just hovers in the air maintaining

its position.

- Open hand: it is detected when all five fingers are extended, as if gesturing stop, and makes the drone land at its current position.
- Fist: it is detected when all five fingers are folded and makes the drone arm and takeoff. If the drone is already in the air nothing happens.
- Index finger pointing up: it is detected when only the index finger is extended and it is pointing roughly towards the top of the image (± 30 degrees) and makes the drone go into offboard mode, where it is possible to receive direct velocity commands.
- Index finger pointing to the right: same as above but pointing to the right of the image and makes the drone roll towards its right side at a speed of 1 m/s.
- Index finger pointing to the left: same as above but the drone rolls towards its left side.
- Thumb pointing to the right: it is detected when index finger is extended up (to maintain the drone in offboard control) and the thumb is extended pointing towards the right of the screen. This gesture makes the drone pitch forward at a steady speed of 1 m/s.
- Thumb pointing to the left: same as the previous gesture, but the drone pitches backward when the thumb point to the left of the screen.

Polish: make sure explanation matches behavior after any code changes

Figure 3.17: Clean-up screenshots of detected gestures with drawn landmarks over hand and no background

The program execution is described in figure 3.18. After all the necessary options have been set, one new thread is started to run the pilot queue loop detailed in 3.3.1, which waits for new commands. On the main thread, the GUI loop runs endlessly until the user quits the program, queuing actions based on gestures calculated from retrieved images and on user input on the keyboard.

Figure 3.18: hand solution loop diagram (MIRO)

3.5 Final solution: human following

The intention behind the development of a UAV control solution that implements tracking and following of humans is to show how the PX4 open-source development platform and

Figure 3.17: Gestures detected by the program to control the movement of the drone

Figure 3.18: Execution flow for the running loop in the hand-gesture control solution.

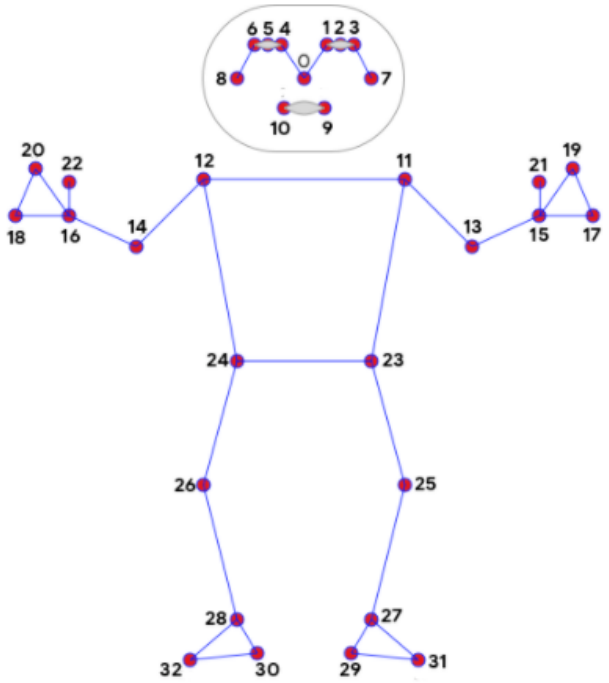

0. nose
1. left_eye_inner
2. left_eye
3. left_eye_outer
4. right_eye_inner
5. right_eye
6. right_eye_outer
7. left_ear
8. right_ear
9. mouth_left
10. mouth_right
11. left_shoulder
12. right_shoulder
13. left_elbow
14. right_elbow
15. left_wrist
16. right_wrist
17. left_pinky
18. right_pinky
19. left_index
20. right_index
21. left_thumb
22. right_thumb
23. left_hip
24. right_hip
25. left_knee
26. right_knee
27. left_ankle
28. right_ankle
29. left_heel
30. right_heel
31. left_foot_index
32. right_foot_index

Figure 3.19: Landmarks extracted from detected human figures by the MediaPipe Pose solution

Source: Adapted from *Pose - mediapipe* [18]

its related projects, MAVLINK and MAVSDK, can be used to design complex real-life applications without the need for expensive state-of-the-art proprietary hardware. The only requirements of the follow application are a PX4-enabled flight controller installed in an aerial vehicle, a companion computer of appropriate dimensions to be able to be mounted on board the vehicle and any camera that can be connected to the companion computer via USB. During the program execution, the drone can be controlled via an RC controller, an external ground station application or keyboard input directly to the companion computer through, for example, a secure shell using the SSH protocol.

For safety, the follow mechanism only engages when the flight mode on the vehicle is changed to offboard mode e.g. by activating a configured switch in the RC controller and stops automatically if the connection to the computer is lost or any of the available failsafes are triggered, like low battery, loss of RC or GPS signal or vehicle attitude exceeding a predefined pitch and roll value for longer than a specified time. In this mode, the vehicle will attempt to find a single person in its field of view and follow their movements by changing its yaw and forward velocity to match horizontal movements and distance changes, respectively.

During the program execution and while the offboard mode and the follow mechanism is engaged, the system continuously retrieves images from the offboard camera that are fed into the MediaPipe Pose [4] computer vision library to extract pose landmarks from it in

Figure 3.20: Valid and invalid poses detected by the follow solution

the form of 2D coordinates. Figure 3.19 shows the available extracted features and their correspondence to the human body. These coordinates are used to draw a bounding rectangle around the detected person and to validate that the received landmarks match the general pose of a person standing up. Figure 3.20 shows some examples of the validation checks being run on the raw landmarks extracted from an image. To prevent unwanted movements, the vehicle will always stop and hover every time it becomes impossible to detect a person in the image received or its features do not match the expected geometry. After a valid bounding box has been defined around the target person, its position with respect to the camera's field of view is sent to a control mechanism composed of two independent PID controllers. The theory behind these controllers is explained in section 3.5.1.

Figure 3.20: valid and invalid person detection from simulator camera output

The first of the PID controllers is in charge of controlling the yaw velocity of the vehicle to respond to horizontal movements in the x direction of the image. It takes as input the x coordinate of the center point of the bounding box, and its target is the middle point of the screen. This controller, therefore, will output velocity commands aimed at maintaining the bounding box centered horizontally in its field of view. The second PID controller controls the forward velocity of the vehicle to respond to distance changes of the person getting closer or farther away from the drone. It takes as input the height of the calculated bounding box as a percentage of the total height of the field of view and works to keep it within a value that matches the desired distance to maintain between the person and the vehicle by moving forwards when the height is too low and backwards when it is too high. The exact percentage of the image height that is covered by a person at a given distance depends on the camera used and needs to be obtained empirically for each separate video source. Figure 3.21 shows how these two inputs are extracted from the coordinates of the bounding box detected around the figure.

Figure 3.21: Calculation of horizontal position and height of figure from the detected bounding box

Figure 3.22: Execution flow for the running loop in the follow control solution

Figure 3.21: Draw calculations over extracted pose from simulator

A summary diagram of the structure of the follow solution can be seen in figure 3.22. After connecting to the pilot module according to the starting options, a loop runs continuously until the user quits the program. For each execution, a new image is retrieved, pose features are extracted from it, and a bounding box is calculated. Then, and only if the vehicle is in offboard flight mode, the calculated positions will be fed into the PID controller to get a velocity output to send to the pilot. Keyboard control is also available to send manual commands to the vehicle directly.

Figure 3.22: follow loop diagram

3.5.1 PID tools

Two additional utilities have been developed for tuning and measuring the performance of the PID controllers. These tools are used in section 4.2 to empirically set the correct values in the coefficients for the controllers. A proportional-integral-derivative is a control loop mechanism commonly used in control systems requiring continuously modulated control. It works by constantly calculating an error value from the difference between the received input on a chosen process variable, which in this case is the detected position of a person in a the frame, and the desired set point for that variable, a position centered in the frame. From the error value, and output for the controller is calculated according to this equation:

$$u(t) = K_p e(t) + K_i \int e(t)dt + K_d \frac{de(t)}{dt} \tag{3.1}$$

where: $u(t)$ = PID control variable
K_p = proportional gain
K_i = integral gain
K_d = derivative gain
$e(t)$ = error value
de = change in error value
dt = change in time

The PID controllers used in this project are developed from the freely-available `simple-pid` library for Python [1]. which provides all the necessary error calculations already implemented. It is only necessary to provide the coefficients, or tunings, and the set point for the controller and then call it periodically with an updated input value to receive the output.

Since the coefficients for a controller are most simply decided empirically, a small tool has been developed to help with the process. With it, it is possible to specify a range of potential coefficients and test the response of the system on the images retrieved from AirSim and a simulated flight controller (either SITL or HITL can be used). For each of the values to be checked, the simulated person to be followed starts in an offset position from the target center, then the controller is engaged with the test values and its detected position input and calculated velocity output a plotted in a graph for analysis. Finally, the vehicle moves back to the starting position to reset the environment for the next value to be checked. The tool is run with the following command: `dronecontrol tools tune`, and can be started with the option `-yaw` or `-forward` to decide which specific controller should be tuned. The other one is deactivated during the test to visualize the effect of the examined values more easily. Each of the coefficients is tested separately by providing fixed values to the other two parameters.

The second tool designed to check the controllers' performance works in a slightly different way from the previous one. The underlying process is the same: engage the con-

troller in an offset position and wait until the movement has stopped before resetting and running again. However, the objective of this tool is to show how an already tuned controller reacts to different position inputs for the camera. The parameter coefficients then remain the same for the entire test and it is the relative position between the vehicle and the followed person that varies. During the execution, both the yaw and the forward controller are activated simultaneously to obtain results closer to what will be expected during actual flight. However, the test tool can be run in either yaw or forward mode, then the distances to be tested between the vehicle and the person vary either left to right or closer to farther, respectively. The objective is to be able to measure how the vehicle will react to increasingly bigger differences to the target position, to ensure that the movement is stable and safety is maintained during the entire flight. A full execution of this tool for both modes is shown in section 4.2.3.

3.5.2 Safety mechanisms

The Dronecontrol application implements a very experimental vision-based guidance system. Therefore, to be able to carry out flight tests with real-life conditions it is necessary to make sure that both the software implements sufficient safety mechanisms so that accidents can be prevented. Some of these guards employed are part of the developed code and others are activated simply from the PX4 safety configuration.

In the first place, the computer vision module prevents accepting as valid input persons that may have been detected wrongly by the computer vision algorithm. The method to determine this is to only accept detected feature points that have a minimum resemblance to a standing human pose, with a taller than wider bounding box and the features for head, shoulder, hip, knee and ankle always stacked from top to bottom in that order. If any of this checks are failed, as well as if there is no detection at all in the image from the algorithm, the vehicle will go into Hold flight mode, which discards any possible pending velocity commands and makes the drone hover over its current position.

The second safety mechanism relates to the PID controllers and pilot module, and consists of limiting the maximum possible velocity of the vehicle at any point during flight. This is done both inside the Dronecontrol application, by setting up output limits on the PID controllers that prevent the guidance system from sending abnormal velocity commands to the flight controller, and from the PX4 autopilot itself as a fallback in case of issues with the custom MAVLink integration or the companion computer as a whole, by setting the `MPC_XY_VEL_ALL` parameter in the autopilot configuration which limits the overall horizontal velocity of the vehicle.

Other safety configuration options included as part of the PX4 autopilot detect undesired behaviour in the flight conditions and trigger a flight mode change to either Hold (hover) or Return (fly back to takeoff position and land), as documented in *Safety Config-*

uration (*Failsafes*) | *PX4 User Guide* [30]. Some of the detected failure conditions are:

1. Lost connection to companion computer while in Offboard mode.
2. RC transmitter link lost while in manual modes, which can be extended to trigger in Offboard mode.
3. Lost GPS position, when the quality of the PX4 position estimate falls below acceptable levels.
4. Low battery during flight.
5. Vehicle unexpectedly flips. (CBRK_FLIGHTTERM)

The last safety mechanism to mention is not based on automatic detection by the developed software or the autopilot, but on active surveillance of the systems behaviour during flight by an operator in control of the vehicle. With an RC controller configured with a switch to control flight mode, it is possible to deactivate Offboard mode at any moment, which will disregard all instructions from the companion computer, and assume full control of the vehicle either through a GPS-assisted mode or completely manual. A secondary switch in the RC controller can be configured as a kill switch for the last-resort option to immediately stop all motor outputs.

Chapter 4

Experiments and validation

This chapter explains the complete process of validating each separate piece necessary for the correct operation of the full system, from testing the first simulation steps to carrying out thorough flight tests on the final guidance solution. Figure 4.1 shows in order each of the steps followed during this validation process.

In the first section, the application is tested in a purely simulated environment, first individually on each part and finally integrating the flight mechanics simulation with providing images to the computer vision detection software with sending control commands to the flight controller simulation. In the second section, the follow detection and guidance solution is tested thoroughly to guarantee that only safe velocity commands are outputted from the PID controllers for any image input that could be received and that their response is according to the desired movement of the vehicle. In the third section, once the software is guaranteed to operate inside the required safety parameters, the simulation is shifted to the dedicated hardware that will be used for real flight: the dedicated autopilot board and the companion computer that will be onboard the vehicle; to ensure that all the connections are working as expected and the devices offer the necessary performance. In the fourth and final section, several flight tests are executed with increasing complexity, from the basic controlling of the vehicle with an RC controller to fully autonomous flight with target following.

4.1 PX4 SITL simulation and validation

Section 3.1 describes the software-in-the-loop simulation mode developed by PX4. By using this mode, it is possible to test and validate the correct operation of each individual part in the program's architecture. To begin with, it is necessary to validate that it is possible to use the connection between the simulated flight controller and the dronecontrol program

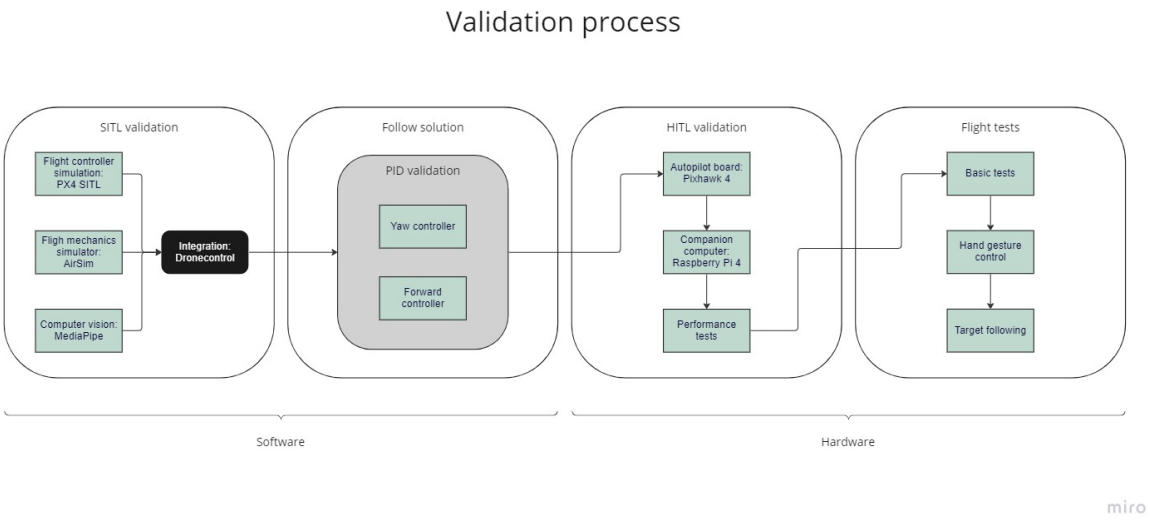

Figure 4.1: Outline for the validation process

to send commands to the simulated vehicle, as well as being able to capture images from a connected camera and use them to test the detection algorithm. The full list of validation steps is therefore:

1. Verify that it is possible to start the simulated flight controller and that it connects to the 3D simulator vehicle.
2. Connect the dronecontrol program to the flight controller and send basic commands.
3. Retrieve images from a camera and run computer vision detection on them.
4. Integrate the last three steps by running the hand-gesture control solution described in section 3.4

For this purpose and to be able to run with a minimal configuration, the Gazebo simulator [1] included with the base PX4 installation will be used as the 3D environment. This simulator works inside Linux in the same computer that runs the SITL PX4. To be able to later transition into using the AirSim simulator instead, which runs in Windows, with minimal changes, for this test PX4, Gazebo and the dronecontrol program will run inside the Windows Subsystem for Linux. The complete installation process necessary to run these tests is explained in appendix A.1 and A.2.

Once both parts are installed, PX4 and Gazebo can be started by running the `make px4_sitl gazebo` command inside its installation folder. The result of this command can be seen in figure 4.2, where the left part shows the user interface and 3D world of the Gazebo simulator and

[1] https://gazebosim.org/home

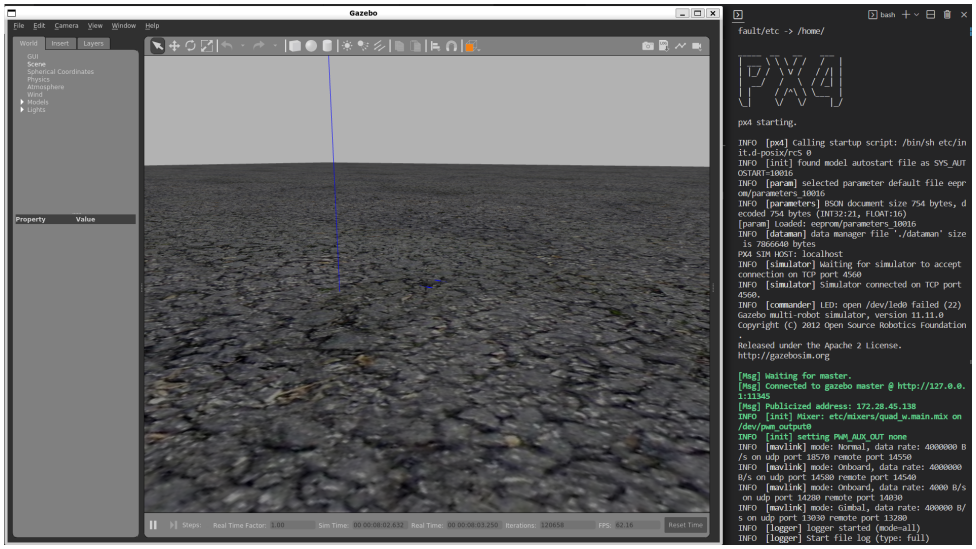

Figure 4.2: Gazebo simulator (left) and output from the PX4 terminal (right) after PX4's software-in-the-loop mode is started

the right side contains the PX4 console that can be used for sending commands and changing the configuration parameters of the simulated flight controller. The simplest command to test is takeoff, which is done by sending `commander takeoff` through the console. Figure 4.3 shows the state of the simulator after the takeoff command, with the vehicle model having climbed to the default height of 2.5 meters above ground. To land the vehicle again, the command is `commander land`.

The next step is to connect the dronecontrol application. The camera testing tool described in section 3.3.3 has been developed for this test, so that it is possible to establish a connection to PX4 SITL and process images without engaging any of the program's control modules. The commands are then sent to PX4 through keyboard input, for example, the key "T" can be used to make the simulated vehicle take off. Figure 4.4 shows the image and text output of the program when the test camera tool is run with the hand detection feature activated. On the left side, the detection algorithm tracks the joint of the hand present in the captured image and on the right side the logged information shows when the connection is established and keyboard commands are sent to the simulator.

Figure 4.4: Get a better image for this

The full execution of a test of the hand-gesture based control solution is shown in video in this link and excerpt of it can be seen in figure 4.5.

Video: Record video of hand-gesture solution running on SITL (+ screenshot on figure 4.5)

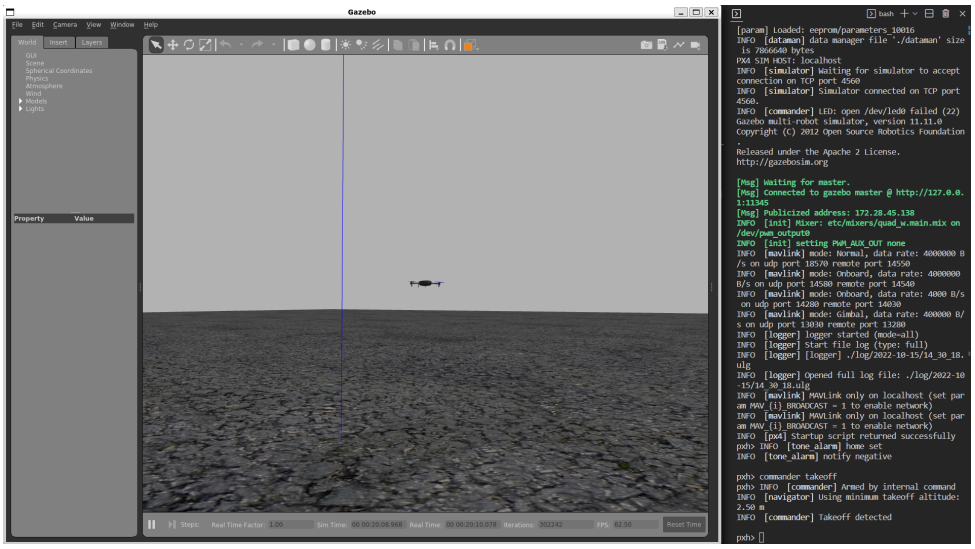

Figure 4.3: Gazebo simulator (left) and output from the PX4 terminal (right) after the takeoff command has been executed

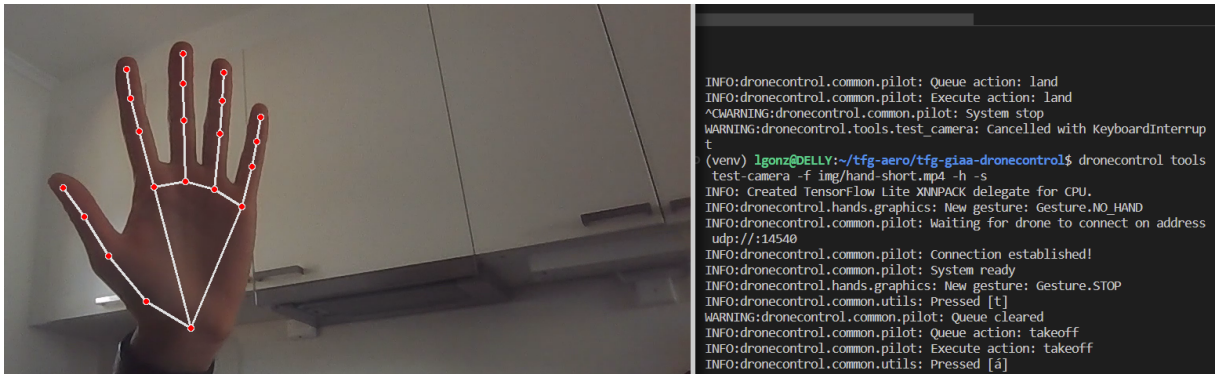

Figure 4.4: Hand detection algorithm running on images taken from the computer integrated webcam

Figure 4.5: Single frame from the video showing the full execution of the hand-gesture control solution

4.1.1 PX4 SITL validation with AirSim

The end goal for the testing environment is for it to use the AirSim simulator to be able to take advantage of its 3D-world and computer vision capabilities. For this reason, it becomes necessary to validate that the new simulator can run correctly on Unreal Engine on the computer and interact with PX4 as well as it did with the default Gazebo simulator and that all the necessary features for detection, tracking and following work as expected. All these characteristics will be checked in the order below:

1. Verify that the AirSim simulator is able to start, connect to the PX4 SITL through the WSL virtual network and receive commands from the PX4 terminal.
2. Check that the dronecontrol program can connect to both AirSim through the WSL network to receive images and PX4 through the local network to send movement commands.
3. Test the pose recognition algorithms on the images obtained from the AirSim simulation.
4. Check that the follow solution is able to control the velocity of the vehicle directly in PX4's offboard mode.

In the first place, the AirSim simulator needs to be installed in the Windows host. The full installation process is described in appendix A.3. There are specific configuration parameters that have to be set to be able to connect the AirSim simulator in Windows to the PX4 SITL running inside WSL. On the simulator side, AirSim's settings file has to include

Figure 4.6: AirSim environment connected to PX4 flight stack running in SITL mode

a line defining the IP address of the network interface to use. This parameter, along with the full configuration file used for SITL testing can be found on appendix A.4. On the PX4 side, it is necessary to specify that the simulator will attach through a different IP address than `localhost`. This is done by setting the `PX4_SIM_HOST_ADDR` environment variable in the Linux system to the IP address of the Windows host on the WSL virtual network before starting PX4 as follows:

```
export PX4_SIM_HOST_ADDR=[IP-address]
make px4_sitl none_iris
```

This starts the software-in-the-loop execution, which attempts to attach to an already running simulator listening on the IP address specified and the TCP port 4560, in this case, AirSim. Therefore, every time one of PX4 or AirSim stops its execution, both of them have to be restarted in the specific order of first the AirSim simulator and then the PX4 flight controller. Figure 4.6 shows the testing environment after the AirSim simulator and the PX4 console have been started successfully.

Figure 4.6: Screenshot of PX4 console + Unreal with Airsim scene

At this point, it is possible to use the PX4 console to send takeoff and land commands to the simulator and observe the 3D-model of the vehicle climb into the air. To test the detection and tracking of human figures from images taken inside the simulator, one can again use the camera testing tool provided with dronecontrol. Figure 4.7 shows the output when the tool is run with the command `dronecontrol tools test-camera --wsl --sim --pose-detection` and a 3D model of a person is situated in front of the drone in the simulated world. In the image, the computer vision utilities detect the main features of the human body and a

Figure 4.7: AirSim, PX4 and dronecontrol applications running side-by-side and connecting to each other

bounding box is drawn around it. Meanwhile, the logged output from the program shows two calculated positions in the terminal: the x coordinate of the mid point of the bounding box and the percentage of the image height covered by the height of the bounding box. These two numbers are the inputs for the PID controllers used in the follow solution as described in section 3.5, so that the output can be used to calibrate the distance from which the drone is to follow the person when that control mode is engaged.

Figure 4.7: dronecontrol console + Unreal with Airsim scene + image output running test-camera

Now that the testing environment is working as expected and before it is used to tune the PID controllers in the follow solution to the response of the vehicle's movement in the next section, it is possible to verify that the controllers are capable of reacting to changes in the position of the figure by only enabling their proportional term with an appropriately low magnitude to keep the movement slow and smooth. The drone movement when running the follow control program with values of 10 and 2 on the proportional term of the yaw and forward controllers, respectively, which can be done with the command `dronecontrol follow --sim --yaw-pid (10, 0, 0) --fwd-pid (2, 0, 0)`, is shown in video format in this link and a frame extracted from it can be seen in figure 4.8.

Video: Record video of follow solution running on AirSim + SITL (+ screenshot for figure 4.8)

Figure 4.8: Single frame from the video showing the movement of the drone in response to changes in position of the tracked person

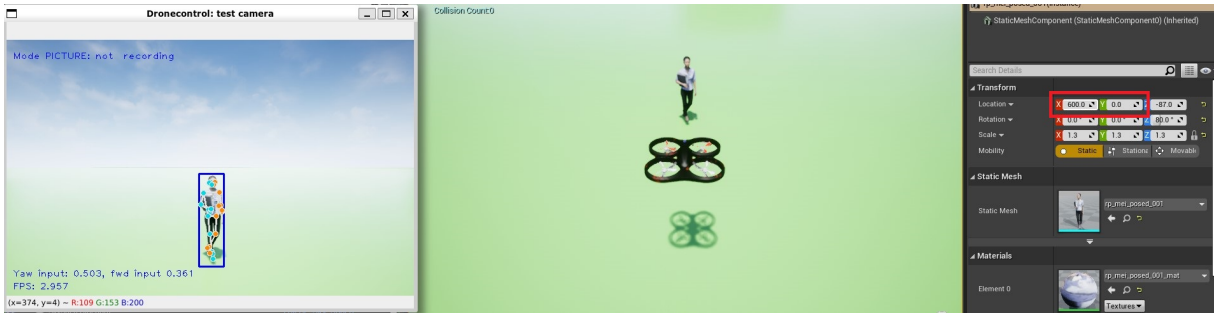

Figure 4.9: Reference position for the yaw and forward PID controllers. From left to right the panels show the dronecontrol application window, the AirSim simulator world view and the world location of the human model in the simulator. The distance between the vehicle and the person is 600 units in the x direction and 0 units in the y direction.

4.2 PID controller validation

´

Video: record tune tool

As has been mentioned before, the velocity controller that is the heart of the person following mechanism is based on two PID controllers. In order to get velocity outputs for the PID controllers that produce a stable movement of the vehicle, it is necessary to tune the parameters of the controllers until the appropriate combination is found. In this section the value for the coefficients used for the project will be found empirically with the help of the tuning tool described in section **??** and developed for this purpose, and its performance validated with the controller testing tool, both running in the simulated environment with the flight stack in SITL mode so that it is possible to take continuous measures of the response of the PID controllers to step movements of a simulated person present in the 3D world. In the first place, each of the controllers will be tuned independently of the other by allowing the vehicle only one direction of movement at a time. Afterwards, both controllers are engaged at the same time to take measurements of their joint response to a range of different inputs.

The controllers are calibrated for a reference position of x=0, y=0 for the vehicle and x=600, y=0 for the person in world coordinates of the simulated environment. At these positions, processed images taken from the simulated camera detect the person centered in the field of view and with a height of 36% of the image height. Which means that the controllers running in the simulator will have as their target set points 0.5 for the yaw controller and 0.36 for the forward controller. So for any changes in the position of the simulated person the controllers will send velocity commands to the autopilot to achieve the same relative position between the vehicle and the person as in the reference shown in figure 4.9.

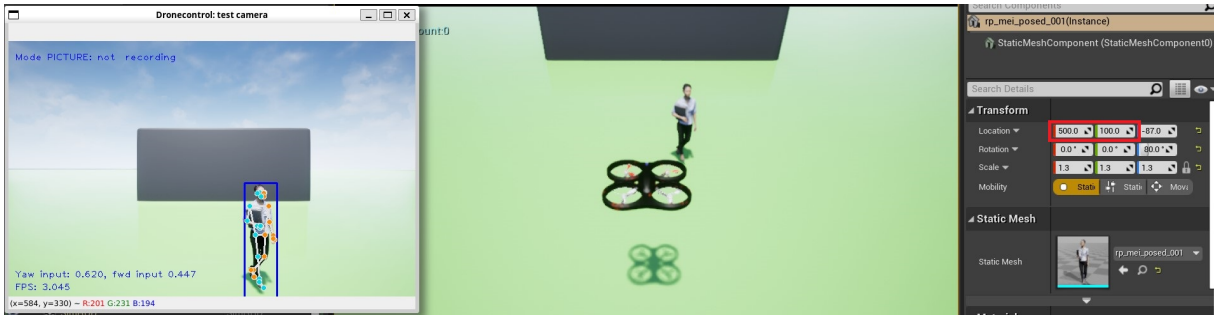

Figure 4.10: Starting position of the simulator for tuning the yaw controller. The human model is situated 500 units forward and 100 units to the right of the vehicle model.

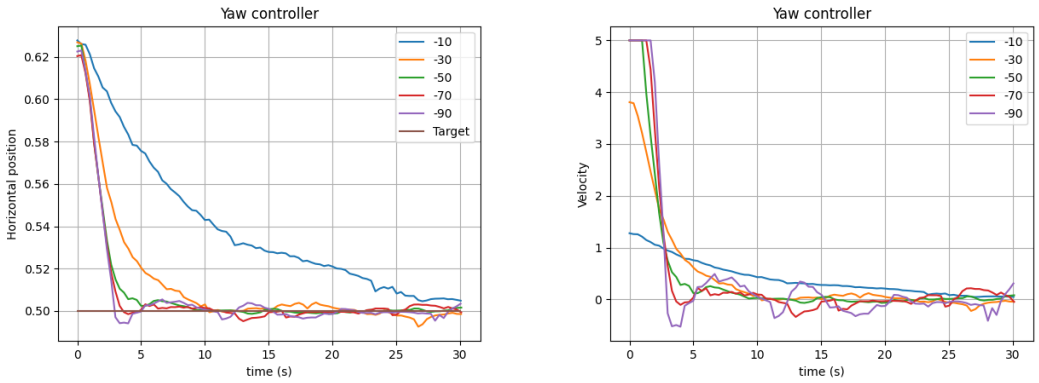

Figure 4.11: Variation of (a) input position and (b) output velocity for different values of K_P and $K_I = 0$, $K_D = 0$ while the yaw controller is engaged.

4.2.1 Yaw controller

To find the correct coefficients for the controller that governs the yaw velocity of the vehicle, the target person is set in a position slightly to the side on its field of view so that when the controller is engaged it produces a rotation of the vehicle to that side. Since the forward controller will not be engaged, the target person can be situated closer to the camera to make it easier for the pose detection algorithm to output correct landmarks. Figure 4.10 shows the starting position of the simulated environment before each run, where the 3D model has been situated at (500,100), that is, 100 units to the right of the reference position. On the left-most panel of figure 4.10, the dronecontrol application shows that the input to the yaw controller is 0.62 at this position. The controller will then need to output a positive yaw velocity to center the person in its field of view. Since this offset position to the right produces a negative difference but requires a positive velocity to counteract, the coefficients for the yaw controller will need to be negative, so that an increased horizontal position results in a positive yaw velocity to decrease it, as indicated by equation 3.1.

To tune the controller to its correct coefficients, the first step will be to test different values of K_P while maintaining K_I and K_D at zero. Figure 4.11 shows the output of the

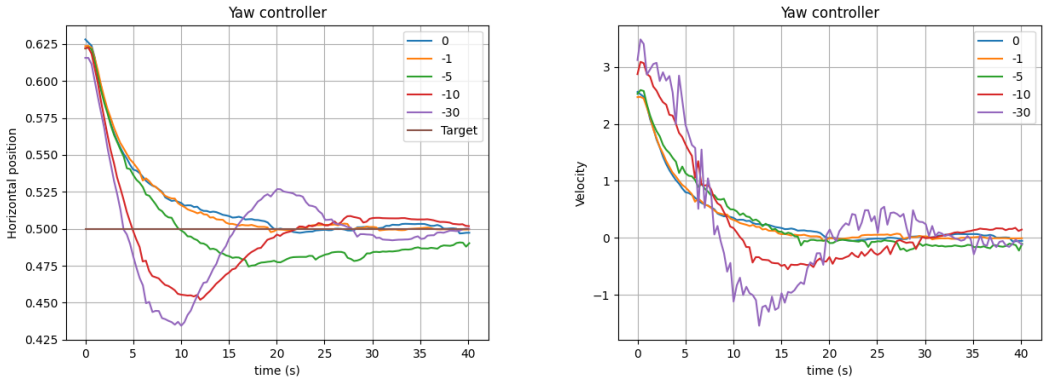

Figure 4.12: Variation of (a) input position and (b) output velocity for different values of K_I and $K_P = -20$, $K_D = 0$ while the yaw controller is engaged.

tuning program for the five values of K_P tested, from $K_P = -10$ to $K_P = -90$ in increments of 20. The left graph represents the variation of the horizontal position detected by the camera for the first 30 seconds after activating the controller and the right graph, the yaw velocity that the controller outputs to the pilot module to reach the target. It can be seen that for low values of K_P, the controller makes the vehicle move slowly towards its target, so that it takes a long time to reach the midpoint position. In the other hand, for high values of K_P the controller tries to reach the target too fast, so when it gets close to it it starts to oscillate around the target. The right side graph also shows well how the output velocity in the yaw controller is limited to 5 degrees per second, so even for very high values of K_P the vehicle will not rotate faster than that. From the graphs, the best of the values tested is $K_P = 50$, where the distance to the target point decreases rapidly (left graph) but the velocity does not start to increase and decrease widely around 0 (right graph).

The second step is to find the correct value for K_I. To do that several values of K_I will be tested for a low K_P of -20 and $K_D = 0$, so that the effect of the integral part is easier to appreciate. Figure 4.12 shows the evolution of the input and output at the controller for a sample time of 40 seconds for each of the values tested. For a low $K_I = -1$, the progress toward the target is stable and slightly faster than without any contribution of the integral part. However, when the K_I increases in magnitude it creates initial oscillations around the target position that fade out as time progresses and, for a very large K_I from around -10 and bigger, the velocity of the vehicle becomes locally unstable with many small variations in its oscillations.

A similar effect can be observed to a lower extent in figure 4.13, where the measurements have been taken for $K_P = -50$ and $K_D = 0$. In this graph, $K_I = -1$ makes the controller reach the target position some 3 seconds faster and with similar oscillations in its velocity than with the proportional part exclusively ($K_P = -50$, $K_I = 0$, $K_D = 0$).

In the last step the tuning process will deal with the derivative part of the controller. In this case, several values of K_D have been tested against the chosen $K_P = -50$ and both

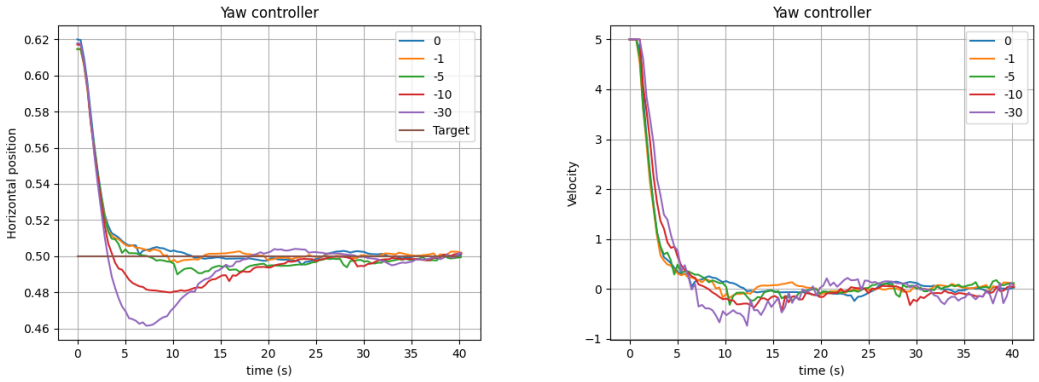

Figure 4.13: Variation of (a) input position and (b) output velocity for different values of K_I and $K_P = -50$, $K_D = 0$ while the yaw controller is engaged.

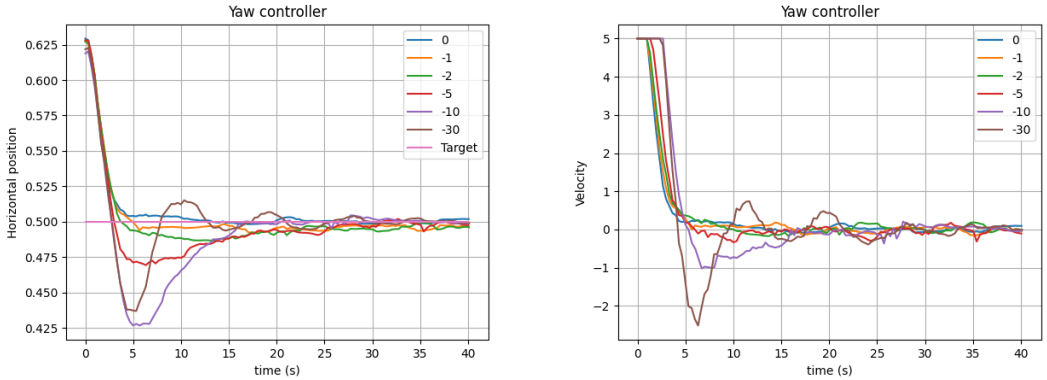

Figure 4.14: Variation of (a) input position and (b) output velocity for different values of K_D and $K_P = -50$, $K_I = 0$ while the yaw controller is engaged.

without any integral part and with $K_I = -1$. This will allow seeing the effect that the derivative part has in the controller as well as validating if the integral part chosen in the last step can work together with the derivative part to make the controller react better to a changed input. Figures 4.14 and 4.15 shows the evolution of the position detected by the computer vision system and the velocity that the controller outputs for a sample time of 40 seconds for $K_I = 0$ and $K_I = -1$, respectively, with $K_P = -50$. For all the tested values, the iteration with $K_I = -1$ on 4.15 shows a better convergence towards the target positions than their counterpart values of K_D for $K_I = 0$, which indicates that the integral part has been chosen correctly. Furthermore, adding any amount to the derivative part does not produce any visible benefit in the step response of the controller and the curve that first stabilizes on the target position continues to be the one for $K_D = 0$, while the velocity graph remains approximately the same between $K_D = 0$ and $K_D = -2$ The final values for the coefficients for the yaw controller will then be $K_P = -50$, $K_I = -1$, and $K_D = 0$, so the controller will in truth only be a PI controller and not a complete PID controller.

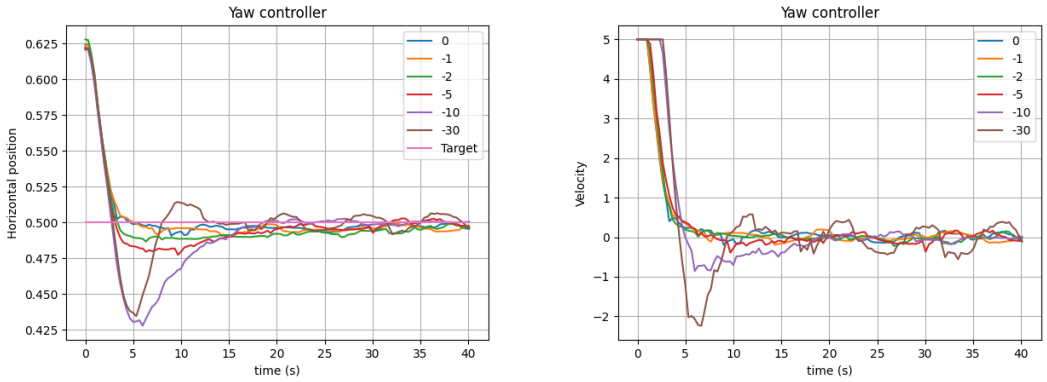

Figure 4.15: Variation of (a) input position and (b) output velocity for different values of K_D and $K_P = -50$, $K_I = -1$ while the yaw controller is engaged.

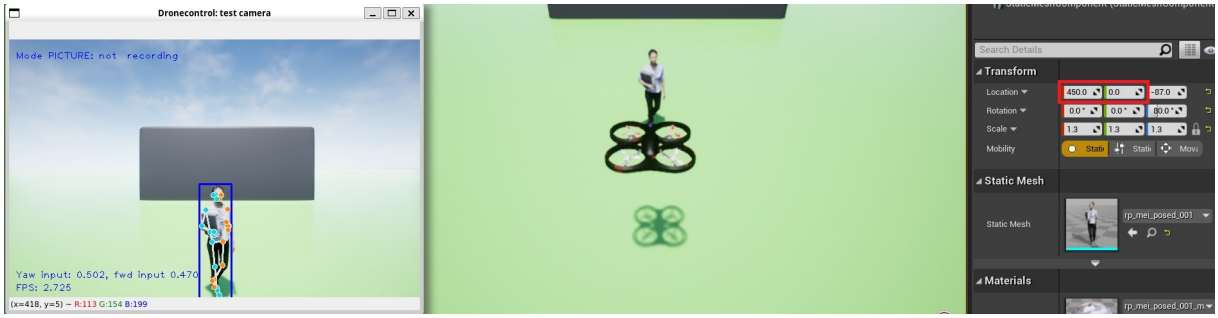

Figure 4.16: Starting position of the simulator for tuning the forward controller. The human model is situated 450 units forward and centered from the vehicle position.

4.2.2 Forward controller

A similar process to the one used for the yaw controller must be followed for the forward controller. The starting position for the tuning process is, in this case, with the figure closer to the vehicle than the reference position and centered in its field of view. Figure 4.16 shows this starting setup with the figure situated at the (450,0) position in the simulated world. In this position, the input to the forward controller is 0.47, that is, the bounding box around the detected figure takes up 47% of the height of the camera field of view. The response from the controller will therefore need to be a negative forward velocity that brings the vehicle away from the target person and reduces the perceived figure height. Since a negative output velocity reduces the input at the entrance of the controller in a directly proportional manner, the coefficients for this PID controller will need to be positive, contrary to what happened on the yaw controller where the feedback loop was inversely proportional (a positive velocity decreased the input to the yaw controller).

In general, the forward velocity will always need to be smaller than the yaw velocity since it induces a pitch angle in the vehicle that tilts the camera up and down which can destabilize the camera and cause a loss of sight of the followed figure. To achieve that, the

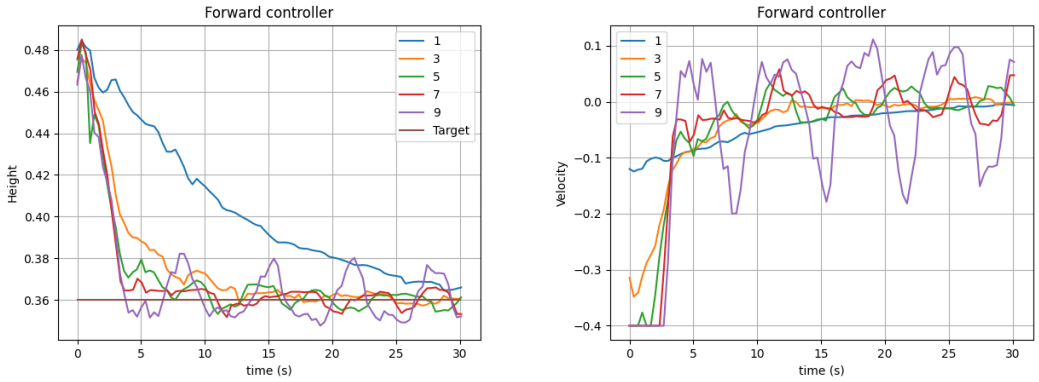

Figure 4.17: Variation of (a) input height and (b) output velocity for different values of K_P and $K_I = 0$, $K_D = 0$ while the forward controller is engaged.

coefficients for the forward controller will be reduced by one order of magnitude. In the first place, values from $K_P = 1$ to $K_P = 9$ in increments of 2 have been tested for $K_I = 0$ and $K_D = 0$ for a sample time of 30 seconds. The curves described by the controller for these coefficients are shown in figure 4.17. In comparison with the trajectory described by the yaw controller, the forward controller is generally more unstable since fast movements forward and backward affect the pose detection algorithm. This is particularly visible at the start of each test as slightly different heights are detected in the image from the camera even though the vehicle is in the same position with respect to the human figure. It also creates an effect, especially for the bigger K_P values tested, where, as the vehicle begins its movement back to its target position, the pose detection mechanism gets a slightly different perspective on the followed person which increases the detected height slightly, so that small spikes of detected differences show in the height graphs even though the velocity graph shows that the vehicle's direction of movement remains the same. This effect is reduced by keeping the output forward velocity small in the controller. In the right graph of figure 4.17, it is also visible for high values of K_P how the output velocity increases enough that the maximum velocity limit is reached on the forward controller and the output is capped to 0.4m/s. For a value up to $K_P = 3$, the trajectory described descends rapidly without ending in big oscillations around the target height, so it is an adequate value to keep for the final controller.

The respective tests for K_I and K_D in the forward controller are shown in figures 4.18 and 4.19. For the integral part, increasing the coefficient causes the controller to overshoot the target initially but then before starting to approximate to the target position. Since for this application, overshooting is not desirable, as it can cause safety issues, the chosen value of K_I will be 0. For the derivative part, every value of K_D testes makes the system increase its oscillations, so it will also be left out of the forward controller. The final values for the coefficients for the forward controller will then be $K_P = 3$, $K_I = 0$, and $K_D = 0$, which makes it only a proportional controller.

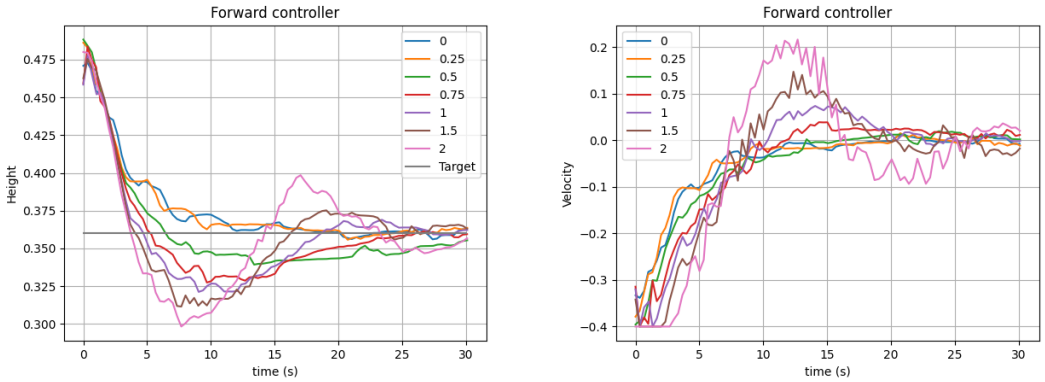

Figure 4.18: Variation of (a) input height and (b) output velocity for different values of K_I and $K_P = 7$, $K_D = 0$ while the forward controller is engaged.

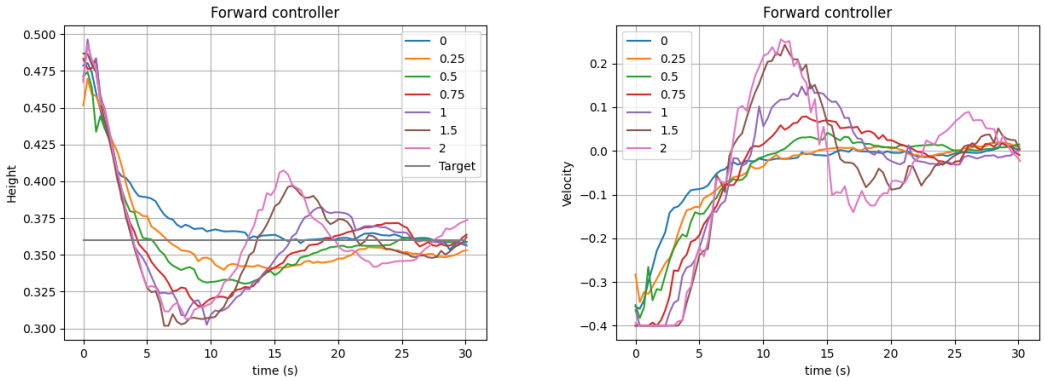

Figure 4.19: Variation of (a) input height and (b) output velocity for different values of K_D and $K_P = 7$, $K_I = 0.5$ while the forward controller is engaged.

4.2.3 PID tuning validation

As a final validation for the tuning obtained previously, in this section the `test-controller` tool described in section **??** will be used check the step response of the controllers to different starting distances for the same coefficients. Additionally, for this test both of the controllers will be engaged simultaneously to verify that work well together. In the first instance, the positions will vary in the y axis, that is, the figure will move from left to right in the field of view of the vehicle. The values for the y coordinate to be tested will be between -150 and 150 units, in increments of 50. The x coordinate of the figure in the simulated world will remain at $x = 500$.

Plots of the changes in normalized horizontal distance and normalized figure height detected by the person recognition algorithm during the time the vehicle takes to reach the target distance from the human figure for each of the positions tested can be seen in figure 4.20. It is considered that the vehicle has reached its target when the error is less than 2% and the output speed at the controller is less than 10% of its maximum. Furthermore, the whole testing process followed with the developed `test-controller` tool can be seen here.

Video: record test-controller tool

Since each of the starting positions differ both in distance and orientation to the target, both of the controllers are engaged to reach it. The yaw controller then introduces a negative yaw velocity when the figure is on the left half of the camera's field of view and a positive yaw velocity when the figure is on the right half to reach the target horizontal distance of 0.5 (figure centered in the image received from the camera); and the forward controller outputs a negative forward velocity to reduce the detected height of the figure from around 0.44 to the target 0.36, since the figure is 100 units closer to the vehicle than the reference position $x = 600$.

Figure 4.20a shows that the most time is spent on starting the movement towards the target and, after that, there is not much difference between the time it takes to reach the -50 position and reaching the -150 position, the former taking 3 seconds and the later taking around 3.6 seconds. In figure 4.20b all of the trajectories have a very similar graph since the starting distance to the target is practically the same, where the controller makes the vehicle pull backwards so the figure stays far enough, making the detected height decrease. For the $y = 100$ starting position the initial detected height is very low for a bit until it reaches the starting point of the other tests, this occurs because the detection algorithm took longer than usual to identify the person. However, after less than half a second, the detection was stabilized without affecting the time it took to reach the target or its final position. This shows that the controllers can recover from errors in the detection mechanism without affecting the movement of the vehicle.

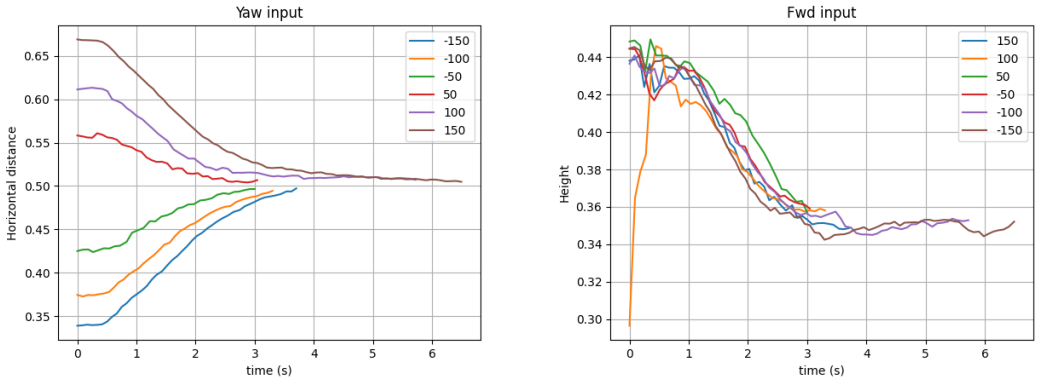

Figure 4.20: Changes over time in detected horizontal position and height as input for the controllers with different starting positions in the y-axis

Additionally, the `test-controller` tool is run with varying positions in the x-axis, which means that the tests are run with the human figure at different distances closer and further away from the vehicle while maintaining in the center of its field of view (y position will remain 0 for the whole process). This means the yaw controller will not need to output any velocity. The changes over time in the input into the forward controller between each starting position and the target position are shown in figure 4.21. The figure reflects that there is a very big difference in how the controller reacts to positions closer and further from the target distance. When the person is very close to the vehicle, there are big differences between detected heights, so the vehicle moves fast away from its position. However, when the person is further away from the vehicle than the target, big differences in distance are detected as small differences in detected height, which causes the controller to output a lower velocity than for the same distance difference when the person is closer to the vehicle and therefore it will take a longer amount of time to reach the target. It is worth noting that even when the person is so close to the vehicle that part of it falls outside of its field of view ($x = 300$ in the figure), the pose detection works well enough to mark where the person should continue outside of the image so that it is still possible for the controller to decide the correct direction of movement.

A video of the complete follow solution running with the appropriate tunings for the controllers can be seen in here.

Video: record follow solution in AirSim with final PID tunings (+ screenshot on figure 4.21)

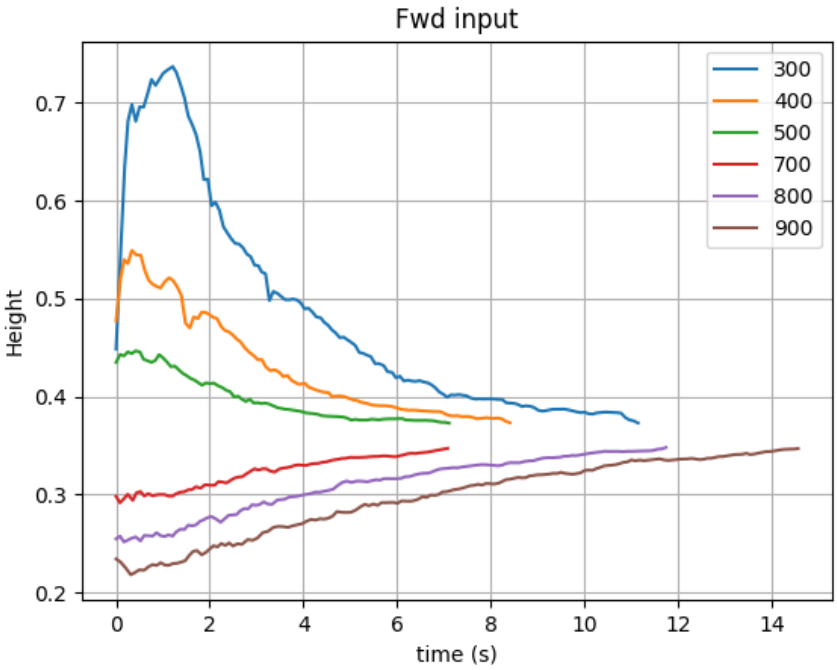

Figure 4.21: Changes over time in detected height as input for the forward controller with different starting positions in the x-axis

4.3 PX4 HITL simulation and validation

The purpose of this section is to validate the transition from using a simulated version of the flight stack running on Linux (PX4's software-in-the-loop simulation) to using a physical Pixhawk board with simulated input and output to test the flight controller interaction with the developed program. To do so, the aim is to be able to run the follow solution to send control commands through the Pixhawk board and observe the movement of the vehicle in the AirSim simulator in the same manner as in the previous section.

To activate this new hardware-in-the-loop mode, QGroundControl contains a specific quadcopter HITL airframe configuration that sets up the board with all the required parameters. QGroundControl automatically detects the Pixhawk 4 board when connected to the computer through its Micro-USB port. It is also required to make changes to the AirSim configuration for the simulator to work with HITL mode, namely, activating the option to accept connections through serial. To test the complete system configuration for HITL described in section 3.1 and outlined in figure 3.5, the Pixhawk board needs an additional channel of communication to the computer dedicated to the Mavlink exchange with the dronecontrol application. The board will therefore have both a direct cable connection to the computer and a telemetry radio on its `TELEM1` port with a wireless link to its counterparty radio connected to the computer. Since the AirSim simulator requires a higher update rate than the dronecontrol application it will employ the faster, cabled link, through which it can automatically connect to the board when it is started. The dronecontrol program will connect through the telemetry radio by specifying the serial port and its baudrate. Since the flight stack is now running on a physical controller, it is possible to add an RC antenna to the `PPM RC` port of the board to be able to fly the vehicle with a remote control unit after it has been bound to the receiver [2]. By configuring one of the switches in the RC unit to change to PX4's offboard flight mode, additional checks to the safety measures of interrupting autonomous flight on flight mode changes or loss of signal from the RC controller can be carried out. Figure 4.22 shows all the connections mentioned.

Figure 4.22: take picture pixhawk hitl + airsim + rc receiver + telem

After all the necessary connections are set up, the program can be started with the following command: `python -m dronecontrol follow --sim --serial COM[X]:57600`, where the exact COM port will vary depending on the particular USB port to which the telemetry radio is connected.

[2] https://docs.px4.io/main/en/config/radio.html

Figure 4.22: Pixhawk 4 board connected to the computer running the AirSim simulator and the dronecontrol application

4.3.1 PX4 HITL validation with Raspberry Pi

The next step in the transition from a fully simulated environment to real flight is to connect the future onboard computer, the Raspberry Pi 4, to the Pixhawk flight controller and proceed with more realistic tests on the exact hardware that will be controlling the drone. The main characteristics of the Raspberry Pi that have to be ensured to be able to progress further towards autonomous flight are:

1. Capacity to function when power is provided from a battery
2. Stability of serial connection to the Pixhawk board
3. Ability to run the dronecontrol application and all its dependencies
4. Connection to an external camera
5. Performance of the computer vision algorithms with reduced processing power

The complete installation process of all the required libraries and dependencies for the Raspberry Pi is explained in appendix A.2.1. The most convenient method of controlling the small computer is through a remote desktop connection, where the screen contents and mouse and keyboard input are transmitted through a local network. This way, it is possible to access the Pi's desktop from the ground station computer even during flight. One option to achieve this is XRDP[3], an open-source implementation of a Microsoft Remote Desktop Protocol server compatible with the Raspberry OS.

[3] http://xrdp.org/

Figure 4.23: Connections between the Raspberry Pi and the Pixhawk board for running the AirSim simulator in HITL mode

The first hardware connection to test is the power supply to the Raspberry. As detailed in section 3.2.3, the selected method for powering the companion computer in the onboard configuration is through a secondary battery. The connection will be done with a USB to USB-C cable, from the battery to the Raspberry Pi, respectively. The intent behind testing the power supply at this point in this process is to verify that it will be suitable for its purpose before it actually needed to power the computer onboard the vehicle. It is necessary that this power source provides enough power to both maintain the processor running at an appropriate speed and provide power to the external camera in turn, which will be attached to the Pi's board and extract power from it.

Figure 4.23: Take picture of pixhawk + rpi with own power supply

A similar connector is used to provide a channel for the Mavlink communication between the flight controller and the onboard computer. In this case, one end of the connector is attached to the `TELEM2` port in the board and the TX/RX pins are attached to the UART pins on the Raspberry's GPIO header. For this serial connection to work, both the flight controller and the companion computer need some additional configuration. The Pixhawk needs to be configured through QGroundControl to enable a secondary Mavlink channel as, by default, only the `TELEM1` port used by the telemetry radio is configured. The necessary parameters to modify and their values are collected in table 4.1. On the Raspberry side, the serial port is configured to be used as a terminal by default. This can be disabled through the `raspi-config` command-line utility (Advanced config -> Serial -> Disable terminal on serial). After that, the `/dev/serial0` address can be used to communicate to the device attached to the UART pins at the baudrate configured through QGroundControl. The `raspi-config` tool and the connector used between the flight controller and the

Figure 4.24: a) Picture of Rpi raspi-config || b) close-up of pixhawk to pi cable connection

companion computer are show in figure 4.24.

Parameter name	Value
MAV_1_CONFIG	TELEM2
SER_TEL2_BAUD	921600

Table 4.1: PX4 parameters than need to be configured to enable Mavlink communication through the secondary telemetry port

Figure 4.24: take screenshot of raspi-config for serial and take picture of rpi pins connection

The test camera utility will be used to validate this configuration. At this point, the only physical connection to the ground station running AirSim and/or QGroundControl is through the development-only micro-USB port in the Pixhawk. The results from running:

```
dronecontrol tools test-camera --hardware /dev/serial0:921600 --sim <AirSim host IP>
↪  --pose-detection
```

can be seen on figure 4.25. On the left side, the remote connection to the Raspberry's desktop shows the output of the dronecontrol program running the pose detection algorithm on the images received from the simulator. On the right side, the AirSim simulator shows the movements of the vehicle as it reacts to the input from the flight controller and the companion computer.

Figure 4.25: take screenshot of rpi desktop and airsim screen while running test-camera in hitl

Figure 4.25: a) RPi desktop with pose output || b) AirSim on Windows

4.3.2 Performance validation

The main question left to answer before the vehicle can take to the air with this hardware and software is whether the less powerful processor in the Raspberry Pi 4b, a quad-core ARM Cortex-A72 64-bit SoC running at 1.5GHz, can handle the detection and tracking algorithms with enough performance to get similar results to those obtained with simulated hardware and achieve good reactions to real-time movement. To do that, the average time that the program spends on each task in the running loop can be calculated and analyzed for different scenarios. Then it will be possible to estimate the maximum speed at which the person being followed by the algorithm can move.

From the follow loop presented in section 3.5 it is possible to divide the processing cost into several sections that can be measured independently: image processing, offboard control, keyboard input, and released thread.

Figure 4.26: draw pie chart of time each section takes for run in airsim + sitl

Figure 4.26 shows the time used for each task on an average run of the follow solution with simulated hardware. The time measurements have been taken by calculating the time difference between the start and the end of each statement and averaging across every run of the loop. The main cost in time of each execution is found in the image processing task,

Figure 4.26: Diagram image for all simulated hardware performance

which takes around 91.8% of the total loop time to run. This is where the most significant differences in performance will come from between the simulated hardware and the solution running in the Pixhawk 4 + Raspberry Pi combination. This image analysis process can be further subdivided to get a finer degree of control over how much time each part takes. The three subtasks that make up image processing are:

1. Get frame: request a new frame from the video source.
2. Process: send the frame to MediaPipe library for detection and/or tracking.
3. Detect: calculate bounding box coordinates and define whether it is a valid pose.

This further division is shown as well in figure 4.26 with each part taking 60%, 30%, and 10% of the total image processing time, respectively, resulting in a performance of around 20 FPS (frames-per-second).

Similar measurements have been taken for hardware combinations with different degrees of simulation, running the follow solution with offboard mode enabled and connected to the AirSim simulator. These are:

1. All simulated hardware: PX4 on SITL mode + dronecontrol on standalone computer + images from AirSim simulator video source.

Figure 4.27: Graph (area??) image for all performance measurements and FPS

2. Simulated hardware with real images: PX4 on SITL mode + dronecontrol on standalone computer + images from attached camera as video source.
3. Test hardware with AC power supply: PX4 on HITL mode on Pixhawk 4 + dronecontrol on Raspberry Pi + images from AirSim simulator video source.
4. Test hardware with battery: PX4 on HITL mode on Pixhawk 4 + dronecontrol on Raspberry Pi powered by battery + images from AirSim simulator video source.
5. Test hardware with real images: PX4 on HITL mode on Pixhawk 4 + dronecontrol on Raspberry Pi powered by battery + images from attached camera as video source.

Figure 4.27: draw graph with each task in the horizontal axis and time in the vertical, one line for each combination

Figure 4.27 shows the measurements taken for all the hardware combinations analyzed.

Write: comment final results from graph

4.4 Quadcopter flight tests

Once the performance and safety of the control algorithms has been validated in the simulated environment, it is possible to begin flight tests and take to the air with a physical drone. In this final section of the validation process, all the previous parts are put together in order to test how the developed software will perform in a real quadcopter during flight. To do this, first it will be necessary to be build the base vehicle from its development kit and then integrate all the additional pieces needed for this project, like the companion computer and the camera. Then, after making sure that the vehicle can fly with all the payload through remote control, both of the developed solutions will be tested: first the hand-control solutions to verify that the autopilot can receive flight commands from an offboard computer and second the follow solution to verify that the companion computer can function as well during flight with its dedicated power supply as it did when it was stationary.

The exact steps that will be executed one after the other to ensure that safety is maintained during the whole process are as follows:

1. Build the quadcopter with its basic components.
2. Add custom payload.
3. Fly with remote control and factory autopilot only, monitoring through QGroundControl.
4. Fly with custom software from offboard computer with `test-camera` tool (3.3.3).
5. Fly with `test-camera` tool from onboard computer.
6. Fly with custom hand-gesture control solution from offboard computer.
7. Fly with custom follow solution from onboard computer.

4.4.1 Build process

As has been mentioned before, the vehicle used in this project is the Holybro X500, designed specifically to work with PX4. The detailed instructions to build the vehicle from its Development Kit can be found in the PX4 documentation [4]. Figure 4.28 shows all the parts that make up the complete vehicle.

After all the standard parts are put together, the custom additions can be attached as well, using the remaining space in the frame. The Raspberry Pi companion computer will

[4] https://docs.px4.io/main/en/frames_multicopter/holybro_x500_pixhawk4.html

Figure 4.28: Development kit for the Holybro X500.

Source: Adapted from *PX4 User Guide* [24].

sit just behind the autopilot to counterbalance the more weighted front of the vehicle where the GPS antenna is located. This location also allows an easy connection between the autopilot and Raspberry's I/O pins with short cables, so as not to clutter the frame with wires excessively.

While in flight, the Raspberry Pi will be powered through a dedicated external battery that outputs power through a 2-ampere USB port. This port will be connected with the Raspberry Pi's original power cable to its USB-C power supply socket. As detailed in 4.3.1, this current is enough to power the connected camera and run the developed software with acceptable performance. This battery will be located underneath the autopilot, centered in the frame of the vehicle, so its weight destabilizes it as little as possible, as can be seen in figure 4.29.

The camera also needs to be attached to the frame of the vehicle in a secure way, with the custom support described in section 3.2.3. The holder attaches to the slide bars underneath the main frame of the vehicle so that the camera and its substantial weight are situated as close to the center of mass as possible behind the GPS platform. The battery powering the engines and the autopilot, which is located on the underside of the carbon frame, is also moved slightly backward from its centered position to make space for the camera and compensate for its weight in the front. Figure 4.30 shows how the underside of the vehicle looks with the camera attached.

Figure 4.29: take picture of complete build and annotate with arrows

Figure 4.30: take picture of underside showing battery and camera holder

Figure 4.29: Complete build of the quadcopter with the main components highlighted

Figure 4.30: Underside of the vehicle, with supports holding the main battery and the camera in place

Figure 4.31: Screenshot from the QGroundControl calibration and setup tools used to configure the vehicle

After the vehicle has been built, there are additional installation and calibration steps that must be carried out before it can fly, also contained in the guide mentioned above. Any simulation modes previously activated for testing must be deactivated from the Safety section of the vehicle configuration and the `MAV_1_CONFIG` parameter set to `TELEM2`, as described in section 3.2.2. Then all the different sensors present, both embedded on the flight controller board and attached to the outside frame, need to be calibrated for this particular build. The QGroundControl 2.2.1 ground station application contains a configuration screen with all the calibration tools needed for the vehicle setup, shown in figure 4.31. The vehicle can be configured either by connecting the flight controller directly to the computer via the micro-USB port on its side or through a wireless connection by plugging the companion telemetry radio into the computer running QGroundControl.

Figure 4.31: take screenshot of sensor config in qgc

4.4.2 Introductory tests

Baseline flight with factory software

Once the vehicle is fully configured, the RC controller and QGroundControl can be used to test assisted take-off and landing. At this point, the drone should be able to maintain stable flight while using autopilot-assisted flight modes like Position Mode, where the roll and pitch sticks control the acceleration over the ground of the vehicle in the forward/backward and left/right directions relative to the heading the vehicle is facing. The throttle controls the speed of ascent and descent. With the sticks centered, the vehicle will actively remain locked to a position in 3D space, compensating for wind and other forces. This is the safest manual mode to test that the standard autopilot works as expected.

Through QGroundControl it is possible to map the different switches in the RC controller to different autopilot commands. For this test, one of the switches with two positions will be mapped to arm/disarm, which controls whether the engines of the quadcopter can start or not; and one of the switches with three positions will be mapped to the landing/takeoff/position flight modes respectively, so the main autopilot modes can be tested by moving the switch between the available positions during flight. This configuration exhausts all the channels available in the RC controller employed. Other flight modes can be set by using the QGroundControl interface directly.

To carry out the flight, first, the main battery is connected to the socket in the power module. This starts up the autopilot, the GPS antenna, the telemetry radio, and the RC receiver. Afterward, QGroundControl can be started on a computer that has been connected to the second telemetry radio via USB. If everything has worked correctly, the ground station application will automatically connect to the vehicle and situate its position on a satellite map. Turning on the RC controller will likewise make it connect to the vehicle, as long as it has been paired correctly, as indicated in the guide linked in the first step of the build process. Once all the wireless connections have been established, the drone can take off by first switching to the armed state and then switching to the takeoff flight mode. While the drone is in the air, switching to the position flight mode will allow direct control through the joysticks in the controller. Figure 4.32 shows an image from a flight carried out following these steps. The full video of the test can be seen here.

Figure 4.32: record video of flight test with RC control (+screenshot for text)

Figure 4.32: Picture from flight tests

Offboard computer flight with test tool

The second test flight will aim to make sure that the custom software can send takeoff and landing commands through a wireless MAVlink channel from the offboard computer (by using the telemetry radio through the developed test tool). For this flight, the QGroundControl application cannot be connected to the vehicle since the telemetry radio channel will be blocked by the custom tool. The RC controller will therefore be used as a backup in case anything goes wrong with the software. At any moment, the controller can switch flight mode and override the input generated from the dronecontrol application, recovering manual control. Since the dronecontrol application can now easily arm the vehicle on its own while sending a takeoff command, the two-way switch of the controller will be mapped for all the tests going forward to the command to kill the power to the engines. This command could be helpful in edge cases to protect the vehicle or the surrounding area if the autopilot were to destabilize during takeoff and landing or completely lose control over the vehicle. Now, once the main battery is connected again to the power module, the test tool is run with the following command for a Windows or a Linux machine, respectively:

```
dronecontrol tools test-camera -r COM<X>:57600
```

or

```
dronecontrol tools test-camera -r /dev/ttyUSB0:57600
```

After a successful connection to the vehicle, the T and L keys in the computer keyboard can be used for takeoff and landing, respectively, and the O key can be used to set the

Figure 4.33: a) Terminal output from the `test-camera` tool running on an offboard computer, b) output from the camera of the offboard computer towards the vehicle in flight

autopilot in offboard flight mode to make it able to receive velocity commands. Afterward, the WASD keys can be used to control the forward and sideways velocity of the vehicle and the QE keys to control its yaw velocity. Figure 4.33 displays the output on the terminal window of the computer, where the connection process and the sent velocity commands are shown, and the output on the camera from the offboard computer.

Figure 4.33: take screenshot from test-camera terminal and image output running for quadcopter + offboard companion computer

Onboard computer flight with test tool

The third and last test flight in this section will ensure that the custom software can send takeoff and landing commands through a cabled MAVlink channel from the onboard computer, as well as making sure that the onboard camera can obtain a good image of the field of view of the vehicle during flight. For that, the same tool will be used as in the last test, but in this instance, it will be run on the Raspberry Pi, and the connection will be established through the wired serial link between this onboard computer and the Pixhawk autopilot board. Since the camera connected to the computer sending commands is now looking down on the pilot, it is possible to activate pose detection on the test images received from this onboard camera. To start the flight test, the main battery and the secondary battery need to be attached, respectively, to the power module and to the Raspberry Pi. After the onboard computer has started up, the easiest way to take control of it is with a remote desktop connection through WiFi, as explained in section 3.1. By this connection, a terminal window can be opened on the desktop, and the following command run:

```
dronecontrol tools test-camera -r /dev/serial0:921600 -p
```

Figure 4.34: Pose detection algorithm running on images taken during flight

As opposed to the flight using the telemetry radio, in this test the serial connection runs at a baudrate of 921600, which matches the configured baudrate on the `TELEM2` port of the Pixhawk board. The "-p" option is used to enable pose detection in the output images. The terminal and camera output can be seen in figure 4.34 and a video recording the remote desktop during the flight can be seen in here.

Figure 4.34: record video of test-camera terminal and image output running for quadcopter + onboard companion computer (+ screenshot for text)

4.4.3 Hand gesture control

During basic flight tests, all the connections and individual parts of the software were validated in real flight. Now it is time to integrate the piloting system with the image recognition results to test the vision-based control solutions developed. The first solution to be used in flight will be the hand-gesture guidance system, as it is made to run on an off-board computer with more available processing resources and no dependence on battery-supplied power to work. The setup will be identical to the second test flight (4.4.2) with the telemetry radio as the serial link and the onboard companion computer turned off Once the autopilot board is powered up, the control solution can be started with the following command:

```
dronecontrol hand -s <device>:57600
```

where <device> is the COM port or TTY device the telemetry radio is attached to, depend-

Figure 4.35: Image taken during flight controlled by the hand-gesture solution. Vehicle is taking off

ing on the platform.

After the pilot connects, the image from the webcam of the computer will appear on the screen with an outline over any detected hand. To start controlling the vehicle, an open palm should be shown to the camera. Then, a closed fist will make the drone take off, and pointing up with the index finger will start the offboard flight mode. Afterward, moving the index finger right or left will make the vehicle mirror the movement, and moving the thumb right or left will make the vehicle move forward and backward, respectively. At any point during the test, an open hand will make the vehicle land at its current place, and losing sight of the controlling hand will make the vehicle return to the starting position before landing as well

Figure 4.35, 4.36, 4.37: record video side-by-side computer screen with terminal and image output and video from vehicle flying, synced, hand solution on windows (+ 3 screenshots of different movements)

4.4.4 Target detecting, tracking and following

Finally, it only remains to test the follow control solution. In this section, the companion computer will be running the follow program and it will be validated whether it is capable of keeping track of and following a moving target during a non-simulated flight. The setup will be identical to the third test in section 4.4.2, without needing a wireless telemetry connection. The telemetry radio is, therefore, free to be used, for example, to track the ve-

Figure 4.36: Image taken during flight controlled by the hand-gesture solution. Vehicle is moving to the right.

Figure 4.37: Image taken during flight controlled by the hand-gesture solution. Vehicle is moving forward

Figure 4.38: Terminal and image output of the dronecontrol follow solution running on the Raspberry Pi

hicle's path through the QGroundControl application on a secondary, offboard computer. The control application will be started with the following command:

```
dronecontrol follow -s /dev/serial0:921600
```

Figure 4.38 shows the process in the terminal of getting the vehicle to takeoff (T key), activating offboard flight mode (O key), and starting movement tracking of the detected figure. The maximum frames per second managed by the program running on the Pi is around In practice, this means that the person being tracked by the drone has to move quite slowly for the camera not to lose sight of them before the autopilot can send the command to the vehicle to move to the previously detected position. At the end of the program run, the average loop time and average runtime for each of the tasks in the main loop are shown in the terminal. From the measures obtained for the test flight carried out, we can see However, for a proof-of-concept scenario, this is an acceptable performance.

Write: Compare performance in follow flight to that in the HITL section

Figure 4.38: same recording as hand solution (+ screenshot from terminal and image output)

Chapter 5

Conclusions

Write: short recap with conclusions

5.1 Evaluation of objectives

Write: Go through objectives in introduction and debate what's been achieved

5.2 Lessons learned

Write: Subsection 1 - cosas aprendidas del grado aplicadas al proyecto

Write: Subsection 2 - cosas aprendidas del tfg en general

5.3 Future work

Write: future work

Appendix A

Installation process

A.1 Installation of PX4 SITL

A.2 Installation of Dronecontrol

A.2.1 Installation on a Raspberry Pi 4

A.3 Installation of AirSim

A.4 AirSim configuration file

A.5 PX4 configuration

A.6 Command-line interface of the Dronecontrol application

Referencias

[1] Martin Lundberg (”m-lundberg”). *simple-pid*. **version** 1.0.1. PyPi. URL: https://pypi.org/project/simple-pid/ (**urlseen** 20/01/2023).

[2] Michael H. („Laserlicht“). *Raspberry Pi 4 Model B - Side*. Wikimedia Commons. URL: https://commons.wikimedia.org/wiki/File:Raspberry_Pi_4_Model_B_-_Side.jpg (**urlseen** 13/01/2023).

[3] R. Bartak **and** A. Vykovsky. **?**Any object tracking and following by a flying drone**? in**cited By 16: 2016, **pages** 35–41. DOI: 10.1109/MICAI.2015.12. URL: https://www.scopus.com/inward/record.uri?eid=2-s2.0-84987776731&doi=10.1109%5C%2fMICAI.2015.12&partnerID=40&md5=fd529a25b1087de90fb4fefdaae0dbf4.

[4] Valentin Bazarevsky **andothers**. *BlazePose: On-device Real-time Body Pose tracking*. 2020. DOI: 10.48550/ARXIV.2006.10204. URL: https://arxiv.org/abs/2006.10204.

[5] V. Bevilacqua **and** A. Di Maio. **?**A computer vision and control algorithm to follow a human target in a generic environment using a drone**? in***Lecture Notes in Computer Science* (*including subseries Lecture Notes in Artificial Intelligence and Lecture Notes in Bioinformatics*): 9773 (2016). cited By 5, **pages** 192–202. DOI: 10.1007/978-3-319-42297-8_19. URL: https://www.scopus.com/inward/record.uri?eid=2-s2.0-84978870802&doi=10.1007%5C%2f978-3-319-42297-8_19&partnerID=40&md5=e627f7ec5cbbf91ae0fa6d9ab2e90927.

[6] P.-J. Bristeau **andothers**. **?**The Navigation and Control technology inside the AR.Drone micro UAV**? involume** 44: 1 PART 1. cited By 316. 2011, **pages** 1477–1484. DOI: 10.3182/20110828-6-IT-1002.02327. URL: https://www.scopus.com/inward/record.uri?eid=2-s2.0-84863704626&doi=10.3182%5C%2f20110828-6-IT-1002.02327&partnerID=40&md5=6ab98e76ba3204cfc101232ba4481a77.

[7] A. Chakrabarty **andothers**. **?**Autonomous indoor object tracking with the Parrot AR.Drone**? in**cited By 27: 2016, **pages** 25–30. DOI: 10.1109/ICUAS.2016.7502612. URL: https://www.scopus.com/inward/record.uri?eid=2-s2.0-

84979779834&doi=10.1109%5C%2fICUAS.2016.7502612&partnerID=40&md5=9c5bd30b53e234b7a03225a07557269a.

[8] T. Chen **andothers**. **?**A Pixhawk-ROS Based Development Solution for the Research of Autonomous Quadrotor Flight with a Rotor Failure**?** **in**cited By 0: 2022, **pages** 590–595. DOI: 10.1109/ICUS55513.2022.9986633. URL: https://www.scopus.com/inward/record.uri?eid=2-s2.0-85146493509&doi=10.1109%5C%2fICUS55513.2022.9986633&partnerID=40&md5=007f69dbcf90b41f45d0f07164e1c382.

[9] J. García **and** J.M. Molina. **?**Simulation in real conditions of navigation and obstacle avoidance with PX4/Gazebo platform**?** **in***Personal and Ubiquitous Computing*: 26.4 (2022). cited By 1, **pages** 1171–1191. DOI: 10.1007/s00779-019-01356-4. URL: https://www.scopus.com/inward/record.uri?eid=2-s2.0-85077550394&doi=10.1007%5C%2fs00779-019-01356-4&partnerID=40&md5=b0e0d31569df60e580c09d395906f34a.

[10] J.E. Gomez-Balderas **andothers**. **?**Tracking a ground moving target with a quadrotor using switching control: Nonlinear modeling and control**?** **in***Journal of Intelligent and Robotic Systems: Theory and Applications*: 70.1-4 (2013). cited By 70, **pages** 65–78. DOI: 10.1007/s10846-012-9747-9. URL: https://www.scopus.com/inward/record.uri?eid=2-s2.0-84871633622&doi=10.1007%5C%2fs10846-012-9747-9&partnerID=40&md5=436e2ed379c01ce7eccc9a1ff66c4369.

[11] K. Haag, S. Dotenco **and** F. Gallwitz. **?**Correlation filter based visual trackers for person pursuit using a low-cost Quadrotor**?** **in**cited By 15: 2015. DOI: 10.1109/I4CS.2015.7294481. URL: https://www.scopus.com/inward/record.uri?eid=2-s2.0-84954554999&doi=10.1109%5C%2fI4CS.2015.7294481&partnerID=40&md5=f9ef86db74cbd24ca7de78ecfc0768c6.

[12] Matt Hawkins. *Raspberry Pi GPIO Header with Photo*. URL: https://www.raspberrypi-spy.co.uk/2012/06/simple-guide-to-the-rpi-gpio-header-and-pins/ (**urlseen** 14/01/2023).

[13] A. Hernandez **andothers**. **?**Identification and path following control of an AR.Drone quadrotor**?** **in**cited By 45: 2013, **pages** 583–588. DOI: 10.1109/ICSTCC.2013.6689022. URL: https://www.scopus.com/inward/record.uri?eid=2-s2.0-84893212045&doi=10.1109%5C%2fICSTCC.2013.6689022&partnerID=40&md5=919fc3ef63f06a24def1d945b196fb81.

[14] Holybro. *Pixhawk 4 - Pinouts*. URL: http://www.holybro.com/manual/Pixhawk4-Pinouts.pdf.

[15] D.M. Huynh **andothers**. **?**Implementation of a HITL-Enabled High Autonomy Drone Architecture on a Photo-Realistic Simulator**? in**cited By 0: 2022, **pages** 430–435. DOI: 10.1109/ICCAIS56082.2022.9990214. URL: https://www.scopus.com/inward/record.uri?eid=2-s2.0-85146419056&doi=10.1109%5C%2fICCAIS56082.2022.9990214&partnerID=40&md5=a05fd463343b8958dc6554fa254c2485.

[16] Anis Koubâa **andothers**. **?**Micro Air Vehicle Link (MAVlink) in a Nutshell: A Survey**? in***IEEE Access*: 7 (2019), **pages** 87658–87680. DOI: 10.1109/ACCESS.2019.2924410.

[17] Google LLC. *Hands - mediapipe*. URL: https://google.github.io/mediapipe/solutions/hands.html (**urlseen** 14/01/2023).

[18] Google LLC. *Pose - mediapipe*. URL: https://google.github.io/mediapipe/solutions/pose.html (**urlseen** 14/01/2023).

[19] J.J. Lugo **and** A. Zell. **?**Framework for autonomous on-board navigation with the AR.Drone**? in***Journal of Intelligent and Robotic Systems: Theory and Applications*: 73.1-4 (2014). cited By 44, **pages** 401–412. DOI: 10.1007/s10846-013-9969-5. URL: https://www.scopus.com/inward/record.uri?eid=2-s2.0-84899426060&doi=10.1007%5C%2fs10846-013-9969-5&partnerID=40&md5=276385022e0f423500563cb9acc4df91.

[20] Microsoft. *Build on Windows - Airsim*. URL: https://microsoft.github.io/AirSim/build_windows/ (**urlseen** 16/01/2023).

[21] A.M. Moradi Sizkouhi **andothers**. **?**RoboPV: An integrated software package for autonomous aerial monitoring of large scale PV plants**? in***Energy Conversion and Management*: 254 (2022). cited By 8. DOI: 10.1016/j.enconman.2022.115217. URL: https://www.scopus.com/inward/record.uri?eid=2-s2.0-85122793867&doi=10.1016%5C%2fj.enconman.2022.115217&partnerID=40&md5=f58a413b75a29d81b49a59e83cc74914.

[22] R.I. Naufal, N. Karna **and** S.Y. Shin. **?**Vision-based Autonomous Landing System for Quadcopter Drone Using OpenMV**? involume** 2022-October: cited By 0. 2022, **pages** 1233–1237. DOI: 10.1109/ICTC55196.2022.9952383. URL: https://www.scopus.com/inward/record.uri?eid=2-s2.0-85143254126&doi=10.1109%5C%2fICTC55196.2022.9952383&partnerID=40&md5=9902a976af40be7654c3a957f8744ea2.

[23] J. Pestana **andothers**. **?**Vision based GPS-denied Object Tracking and following for unmanned aerial vehicles**? in**cited By 66: 2013. DOI: 10.1109/SSRR.2013.6719359. URL: https://www.scopus.com/inward/record.uri?eid=2-s2.0-84894224375&doi=10.1109%5C%2fSSRR.2013.6719359&partnerID=40&md5=b62d374446ced88aebe4e5f875057f52.

[24] *PX4 User Guide*. The Linux Foundation. URL: https://docs.px4.io/main/en/ (**urlseen** 13/01/2023).

[25] Renderpeople. *Over 4,000 Scanned 3D People Models*. URL: https://renderpeople.com/ (**urlseen** 16/01/2023).

[26] R. Rysdyk. **?**UAV path following for constant line-of-sight**? in**cited By 88: 2003. DOI: 10.2514/6.2003-6626. URL: https://www.scopus.com/inward/record.uri?eid=2-s2.0-85088181184&doi=10.2514%5C%2f6.2003-6626&partnerID=40&md5=776e0fc59263d18dbb9bb05d1a360141.

[27] Shital Shah **andothers**. *Aerial Informatics and Robotics Platform*. techreport MSR-TR-2017-9. Microsoft Research, 2017.

[28] PX4 team. Dronecode foundation. URL: https://docs.px4.io/main/en/advanced_config/parameter_reference.html (**urlseen** 17/01/2023).

[29] PX4 team. *Pixhawk 4 - PX4 User Guide*. Dronecode Foundation. URL: https://docs.px4.io/main/en/flight_controller/pixhawk4.html (**urlseen** 14/01/2023).

[30] PX4 team. *Safety Configuration (Failsafes) | PX4 User Guide*. Dronecode foundation. URL: https://docs.px4.io/main/en/config/safety.html (**urlseen** 21/01/2023).

[31] Fan Zhang **andothers**. *MediaPipe Hands: On-device Real-time Hand Tracking*. 2020. DOI: 10.48550/ARXIV.2006.10214. URL: https://arxiv.org/abs/2006.10214.